eng

MDPI

Article

Engineering Properties of Modified Rubberized Concretes: Role of Metakaolin and Ground Blast Furnace Slag as Ordinary Portland Cement Replacements

Zahraa Hussein Joudah * and Baydaa Abdul Kareem

Department of Civil Engineering, Faculty of Engineering, University of Misan, Misan 62001, Iraq; bida.k.z@uomisan.edu.iq

* Correspondence: zahraa.alsafy85@uomisan.edu.iq

Abstract: Discarded rubber tires (DSRTs) have become a significant landfill and environmental problem that needs to be solved to reduce health risks, fires, and other environmental issues. The inclusion of such rubber can enhance the ductility of concrete and increase its resistance to dynamic loads, as well as enhancing the concrete's durability and lifespan by modifying its impact resistance (IR). However, the smooth surface and low bond strength with cement pastes directly lead to a decrease in the strength of the proposed concrete, restricting its range of use in the construction industry. The inclusion of pozzolanic materials with high hydraulic capacity in the concrete matrix as partial cement replacements, such as granulated blast furnace slag (GBFS), has led to enhanced performance of the modified rubberized concretes (MRCs) in terms of bond strength and other mechanical properties. Based on these facts, this study aimed to evaluate the effects of including 20% GBFS and various levels (5–25%) of metakaolin (MK) as replacements for ordinary Portland cement (OPC), on the engineering properties of newly designed rubberized concretes. For this purpose, twenty-two mixes of MRCs were prepared by replacing the OPC and natural aggregates with various contents of GBFS, MK, and DSRTs. The results indicated that the MRC specimens prepared with a ternary blend of OPC-GBFS-MK illustrated significant improvements in strength performance, wherein the compressive strength (CS) after the curing age of 56 days (46.5 MPa) was higher than that of the OPC control mix (41.2 MPa). Moreover, the mix designed with high amounts of MK-GBFS-DSRTs significantly enhanced the engineering properties of the proposed MRCs by increasing the IR and reducing the total porosity. It can be asserted that, by using MK, GBFS, and DSRTs as renewable resources for construction materials, the environmental problems can significantly be reduced, with excellent benefits in the engineering properties of the designed rubberized concretes.

Keywords: DSRTs; MRCs; engineering properties; porosity; ductility

Citation: Joudah, Z.H.; Abdul Kareem, B. Engineering Properties of Modified Rubberized Concretes: Role of Metakaolin and Ground Blast Furnace Slag as Ordinary Portland Cement Replacements. *Eng* **2024**, *5*, 2067–2091. https://doi.org/10.3390/eng5030110

Academic Editor: Božo Smoljan

Received: 30 June 2024
Revised: 16 August 2024
Accepted: 22 August 2024
Published: 1 September 2024

1. Introduction

In the global construction industry, concrete with extreme stiffness or low ductility is often seen as brittle and less useful [1]. Improving the ductility of concrete is a crucial factor in the design of concrete mixtures [2]. Therefore, many supplementary materials are recommended to enhance the strength traits of concrete to meet application requirements [3,4]. The energy absorption capacity or resilience of evaluated concrete is typically regarded as its most crucial characteristic under impact loading. The addition of DSRTs to concrete can enhance its impact resistance (IR), thereby improving its toughness. Numerous studies [5–7] have shown that substituting natural fine and coarse aggregates with DSRTs enhances the overall impact strength of concrete. Studies conducted by Li et al. [8], Khalil et al. [5], and Liu et al. [9] found that replacing the fine or coarse aggregates with 10 to 30% DSRTs significantly improved the concrete's energy absorption capacity and increased its IR value.

Unfortunately, the strength properties of rubberized concrete, such as compressive strength (CS), tensile strength (TS), flexural strength (FS), etc., are inversely influenced by the DSRT content, and the strength decrement increased significantly when the replacement level was increased up to 20% [10]. Several studies [11–13] have noted a considerable reduction in the CS and elastic modulus of MRCs at various levels of rubber waste incorporation. Eldin and Senouci [14] reported the replacement of natural aggregates with several sizes and levels of DSRTs to produce rubberized concrete, resulting in a drop in CS to nearly 65% in comparison to normal concrete. In a study to develop high-performance free cement rubberized concrete by Al-Fasih et al. [15], the authors observed that it was possible to produce high-CS concrete (more than 30 MPa) by replacing the natural aggregates with 30% DSRTs. However, increasing the level of DSRTs up to 30% significantly affected the CS development. In another study conducted by Mhaya et al. [16], it was found that replacing natural aggregates with 10% fine or/and coarse DSRTs can be effective without any loss in the CS of the prepared specimens. Conversely, the proposed concrete lost more than 47% of its CS value when the level of replacement was increased to 30%. The loss in strength properties, especially for the CS, was attributed to the smooth rubber surface, which directly affected the bond strength between the DSRT particles and cement pastes [10,17,18]. Several studies [19–22] have successfully enhanced the adhesion between DSRTs and pastes, obtaining rubberized concrete with acceptable CS by enhancing the OPC's properties utilizing supplementary cementitious materials (SCMs), or by treating the rubber surface using heat or chemical treatments.

Several types of SCM, such as fly ash (FA), ground blast furnace slag (GBFS), and palm oil fuel ash (POFA), are used to develop high-performance MRCs. In [23], the authors reported that the inclusion of POFA as an OPC replacement significantly improved the bond strength between the DSRTs' surface and the cement, while also increasing the CS values. Similarly, the MRCs prepared with GBFS as an OPC replacement at various levels achieved excellent results and significantly enhanced CS [24]. Additionally, nanotechnology was utilized to improve the rubberized concrete's performance, and the nanosilica obtained from waste bottle glass incorporated in the GBFS-OPC binder significantly enhanced the bond strength and increased the strength values of the designed MRCs [25]. Metakaolin (MK) is the anhydrous calcined form of the clay mineral kaolinite and is classified as a type-N SCM, with a very high aluminosilicate composition (more than 90%) [26]. MK powder is widely used as an SCM to improve the strength and durability properties of OPC concrete [27–29]. Given the significant advantages of strength and durability in concretes, high contents of SCMs such as GBFS have been utilized in production to decrease the usage of cement [30] and reactive powder [31]. The concretes containing GBFS demonstrated favorable outcomes concerning hydration [32] and microstructural properties [33], which heavily depended on the reactivity of the GBFS, slag characteristics, resources, raw materials, processes, and cooling rates [34,35]. The global construction industry seeks rubberized concretes for their excellent ductility and impact resistance.

Driven by the potential advantages and suitable chemical composition of GBFS and MK, the novelty of this study is in enhancing the properties of cement by including MK as a GBFS replacement and measuring its effects on bond strength with the surface of rubberized particles. The aims of this study were to determine the optimal content of MK as a GBFS replacement and its effects on the CS development of the designed binders. The effects of ternary blended OPC-GBFS-MK binders and various levels of DSRTs as replacements for fine and/or coarse natural aggregates were widely evaluated in this experiment. Several tests such as CS, TS, FS, and modulus of elasticity (MOE) were adopted to evaluate the MRCs strength performance. In addition, the microstructure tests were conducted to understand the mechanism of hydration process and gels formulation. Finally, to measure the IR of the proposed concrete and address the growing demand for such assessments, various methods with distinct guidelines were employed to evaluate the IR of rubberized concretes. Tests such as the Charpy impact, drop weight, and projectile impact

have been developed. Among these, the ACI Committee 544 recommends the drop weight test as the most prevalent and significant method.

2. Materials and Methods

2.1. Preparation of Materials and Mix Design

In preparing the MRC specimens, a ternary blend of OPC, GBFS, and MK was used as binder. Additionally, different-particle-sized DSRTs were utilized to replace the natural aggregates (NAs) of fine river sand and crushed stone. To determine the chemical composition of OPC, GBFS, and MK, X-ray fluorescence (XRF) spectroscopy was conducted. The analysis results are presented in Table 1. From the analysis results it was found that the calcium oxide and silica oxide are the main compounds, with weight percentage of 67.84 and 17.62, respectively. The contents of aluminum, magnesium, and potassium oxides were found to be much lower, at 4.56, 2.15, and 0.28%, respectively. Likewise, the GBFS was found to be very rich in silica and calcium oxides, which together account for more than 75% of its chemical composition. However, the content of aluminum oxide (13.67%) and magnesium (5.09%) was slightly higher than the OPC. In contrast, the MK sample showed a high weight percentage of silica, aluminum, and potassium (more than 96.5%) with a very low content of calcium oxide (0.08%). It is well known that silica, aluminum, magnesium, and potassium oxides are very important elements in the cement hydration process, improving the gels formulation (C-S-H, C-S-A-H, and C-CO_3) and increasing strength properties of the paste. For this reason, the GBFS and MK are incorporated into the OPC matrix at various replacement levels to enhance its chemical composition by increasing the content of silica, aluminum, magnesium and potassium oxides. Furthermore, the total loss on ignition (LOI) in the GBFS chemical composition (0.24%) was lower than that observed in OPC (1.69%) and MK (1.65%). This was significantly lower than the 1.7 observed in OPC. According to ASTM C618 standards [36], GBFS and MK comprise more than 90% of calcium, silicate, and alumina, meeting the criteria for pozzolanic materials. The physical properties of materials used in this study were also evaluated through tests such as particle size analysis and specific gravity measurement. For the OPC, the median particle sizes and specific gravity were found to be 9.15 μm and 3.17 g/cm^3, respectively. In comparison, the results indicated that the median particle size and specific gravity of GBFS were 11.8 μm and 2.88 g/cm^3, respectively. Similarly, the MK exhibited a higher specific gravity (2.67 g/cm^3) compared to OPC. However, the fine particle size was observed in the MK sample (8.6 μm) compared to 9.15 and 11.8 μm for OPC and GBFS, respectively.

Table 1. Ternary blended binders' materials of OPC, GBFS, and MK: chemical composition.

Materials	SiO_2	Al_2O_3	CaO	MgO	Fe_2O_3	Na_2O	K_2O	TiO_2	MnO	P_2O_5	LOI	Other
OPC	17.62	4.56	67.84	2.15	3.37	0.02	0.28	-	-	0.02	1.69	2.45
GBFS	30.53	13.67	46.02	5.09	0.33	0.24	0.36	0.02	-	0.01	0.24	3.49
MK	52.22	42.18	0.08	0.26	0.49	0.01	1.73	0.01	0.01	0.13	1.65	1.23

The crystalline and amorphous structures of OPC, GBFS, and MK are presented in Figure 1, analyzed using X-ray diffraction (XRD). Figure 1a displays the XRD pattern of the utilized OPC. From the analysis results, it was observed that the low amorphous part of OPC was between 25 to 55 of 2θ degrees. The XRD pattern of OPC exhibits prominent peaks of dicalcium silicate (C_2S), tricalcium alminate (C_3A), and tricalcium silicate (C_3S). Results from the X-ray diffraction (XRD) pattern of GBFS reveal a highly amorphous nature, indicated by the absence of any sharp peaks. As shown in Figure 1b, the XRD analysis found that the major mineral presenting an amorphous structure was quartz (SiO_2). Furthermore, GBFS contains a high amount of amorphous calcium oxide (CaO), which significantly improves the hydration process of modified cement. Therefore, GBFS may contribute significantly to hydraulic capacity and pozzolanic performance due to

its properties, including small particle size, large surface area, and amorphous content. Figure 1c illustrates the XRD of metakaolin, which shows a broad band between 9.8 and 28 2θ degrees and a distinct crystalline peak at 26.8 2θ degrees, indicating a primarily amorphous structure with SiO_2. The sample also contains crystalline phases of mullite, aluminum silicate, calcium oxide, magnesium silicate, and aluminum magnesium. Quartz is generally known to be unreactive, while the presence of muscovite, an impurity from the client, is consumed during the synthesis reaction. The noncrystalline silicate minerals in GBFS have higher reactivity with $Ca(OH)_2$ created from the cement hydration to produce additional C-(A)-S-H gels. This reduction in $Ca(OH)_2$ and the increase in C-(A)-S-H gel content contribute to enhanced strength and the production of more durable concretes.

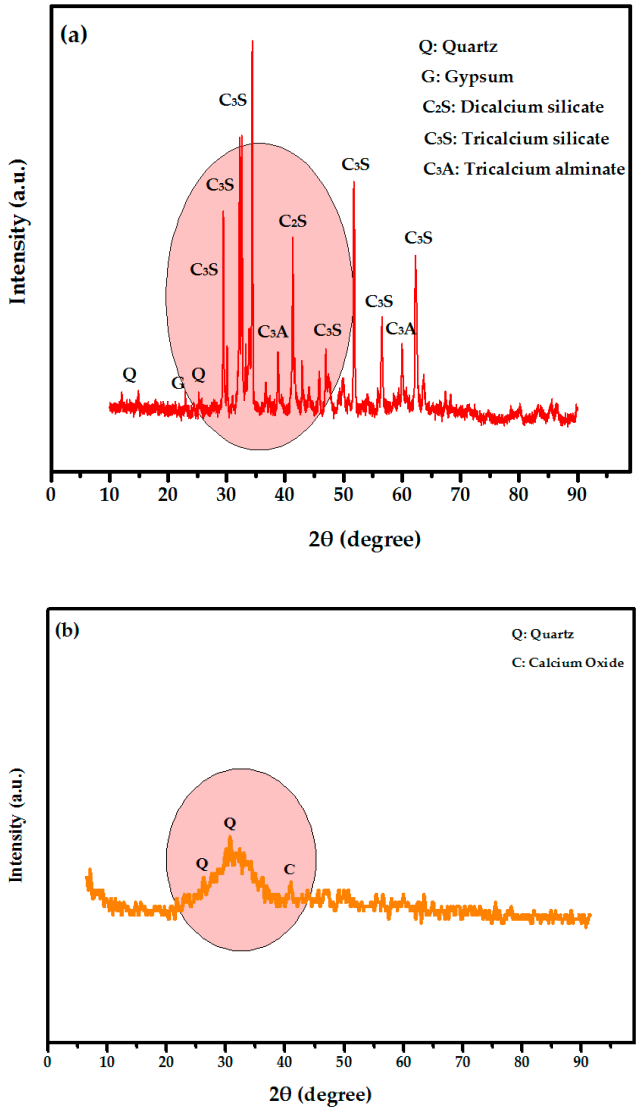

Figure 1. *Cont.*

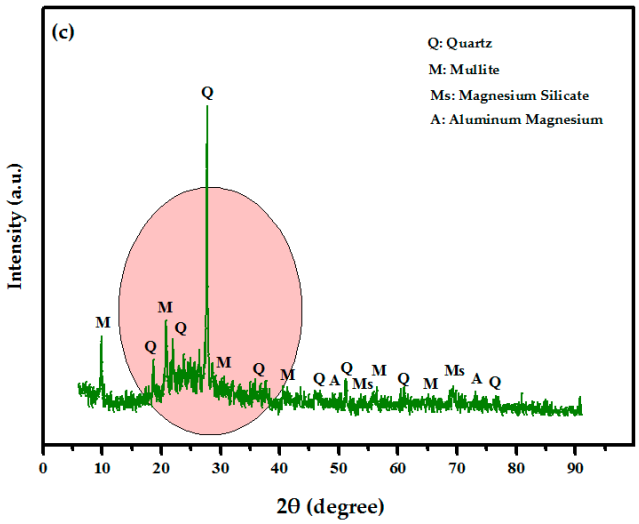

Figure 1. The XRD analysis results of raw materials: (**a**) OPC, (**b**) GBFS, and (**c**) MK.

The MRC specimens were prepared according to ASTM C33 [37], utilizing natural river sand as fine aggregate. Before use, the appropriate water-to-cement ratio was determined by maintaining the sand in a saturated surface dry (SSD) condition, as specified in ACI-219. The absorption capacity and specific gravity (2.7) of the well-graded sand (with a fineness modulus of 2.8) were assessed under SSD conditions. The sand's specific gravity fell within the acceptable range (2.4 to 3.0) but was slightly lower compared to that of the coarse aggregates [38]. The water absorption (2.2%) of the fine NAs (river sand) was within the referenced range (0.2 to 3.2%) [38]. Ground granite stones, free from harmful components such as organic matter, grasses, leaves, dry mud, and silts, were used as coarse aggregates. The specific gravity and particle size distribution of the coarse aggregates were also examined under SSD conditions. Approximately 60 to 80% of the total aggregate volume was used to prepare the concrete mixes, with the maximum particle sizes of fine and coarse NAs being 4.7 mm and 10 mm, respectively. To prepare these aggregates, discarded tires were shredded into small pieces using shredders and shearing equipment. The modified rubberized concretes were prepared using two types of DSRTs (graded by ASTM C136 [39]) with grain sizes ranging from 1 to 4 mm and 5 to 8 mm with specific gravity of 1.3 and 1.4 and water absorption of 0.90 and 0.96%, respectively. However, the contents of fiber and metal were found to be less than 1 and 0.5 weight percentage, respectively. In addition, it was found the rubber hydrocarbon contributed over 50% of the total chemical composition of the DSRTs. However, the ash, acetone extract, and carbon black content contributed 24, 10, and 14%, respectively.

To develop high-performance MRCs, twenty-two mixes were designed with varying content of GBFS, MK, and DSRTs, as shown in Figure 2. Table 2 illustrates mixes used in this study. Firstly, the modified ternary binders were prepared by replacing 20% of OPC by GBFS. Then, different levels of MK (5, 10, 15, 20, and 25%) were added to the cement matrix to determine the optimal replacement ratio. Next, the DSRTs were used as fine aggregates in five mixes by substituting 5, 10, 15, 20, and 25 % of NAs by volume. Additionally, the effect of coarse DSRTs on MRC performance was evaluated by replacing the crushed stone with 5, 10, 15, 20, and 25% of coarse DSRTs. Finally, the fine and coarse NAs were replaced by 5, 10, 15, 20, and 25% of both fine and coarse DSRTs (50:50 ratio). Throughout the process, the water content (w/c ratio) and superplasticizer (SP) were maintained at 0.48 and 0.03, respectively.

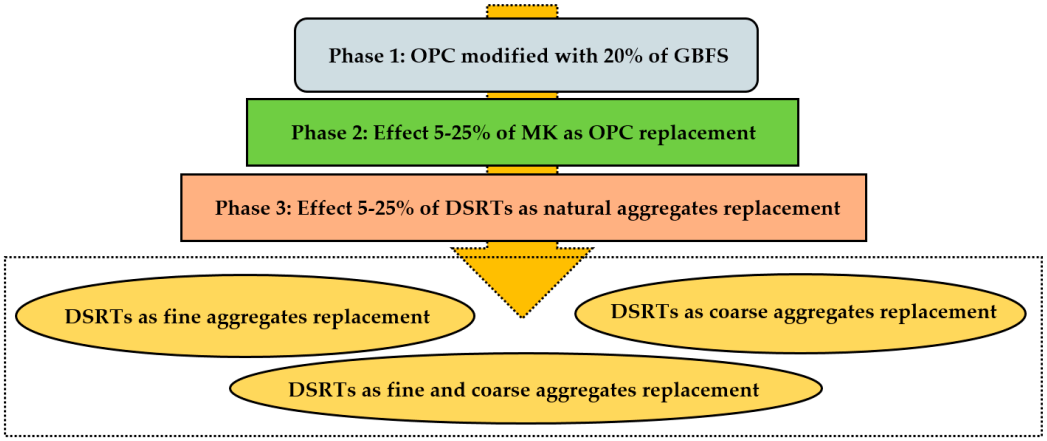

Figure 2. Experimental procedure for modified rubberized concretes.

Table 2. MRCs mix design containing GBFS and MK as OPC replacement.

MRCs' Mixes		Ternary Binder, kg/m^3			w/c Ratio	SP, %	NAs, kg/m^3		DSRTs, kg/m^3	
		OPC	GBFS	MK			Fine	Coarse	Fine	Coarse
Control specimens	OPC	425	0	0	0.48	0.03	825	890	0	0
Modified cement binder incorporating high content aluminosilicate materials of GBFS and MK	GBFS	340	85	0	0.48	0.03	825	890	0	0
	MK5	318.7	85	21.3	0.48	0.03	825	890	0	0
	MK10	297.5	85	42.5	0.48	0.03	825	890	0	0
	MK15	276.3	85	63.7	0.48	0.03	825	890	0	0
	MK20	255	85	85	0.48	0.03	825	890	0	0
	MK25	233.7	85	106.3	0.48	0.03	825	890	0	0
DSRTs as 5, 10, 15, 20, and 25 volume % of fine aggregates replacement	RF5	297.5	85	42.5	0.48	0.03	804.17	890	20.83	0
	RF10	297.5	85	42.5	0.48	0.03	783.34	890	41.66	0
	RF15	297.5	85	42.5	0.48	0.03	762.51	890	62.49	0
	RF20	297.5	85	42.5	0.48	0.03	741.67	890	83.32	0
	RF25	297.5	85	42.5	0.48	0.03	720.84	890	104.15	0
DSRTs as 5, 10, 15, 20, and 25 volume % coarse aggregates replacement	RC5	297.5	85	42.5	0.48	0.03	825	867.17	0	22.82
	RC10	297.5	85	42.5	0.48	0.03	825	844.34	0	45.65
	RC15	297.5	85	42.5	0.48	0.03	825	821.51	0	68.48
	RC20	297.5	85	42.5	0.48	0.03	825	798.68	0	91.31
	RC25	297.5	85	42.5	0.48	0.03	825	775.86	0	114.14
DSRTs as5, 10, 15, 20, and 25 volume % fine and coarse aggregates replacement	RFC5	297.5	85	42.5	0.48	0.03	814.58	878.58	10.41	11.41
	RFC10	297.5	85	42.5	0.48	0.03	804.17	867.17	20.83	22.82
	RFC15	297.5	85	42.5	0.48	0.3	793.75	855.76	31.24	34.24
	RFC20	297.5	85	42.5	0.48	0.3	783.34	844.34	41.66	45.65
	RFC25	297.5	85	42.5	0.48	0.3	772.92	832.92	52.07	57.07

2.2. Specimens Preparation and Curing Regime

The preparation of the MRC specimens involved the ternary binder of OPC, GBFS, and MK being blended in a dry condition for 5 min in a special machine with fast speed. Then, medium concrete mixer was used to prepare the fresh concrete mixtures. Firstly, the fine and coarse NAs and DSRTs aggregates were mixed for 3 min. Later, 50% of the prepared ternary

blended binder of OPC, GBFS, and MK was added and mixed for another 3 min. Then, the remaining 50% of the ternary blend was added gradually and mixed for another 3 min. Finally, the prepared liquid of water and SP were added to hydrate the blend. After mixing the MRCs matrix for 4 min, the freshly prepared MRCs were cast into the mold in three layers. Each layer was reinforced using a vibration table for approximately 15 s to eliminate air voids. Four kinds of specimens (three for each mixture) were made into cubes, cylinders, beams, and disks, measuring (100 mm × 100 mm × 100 mm), (100 mm × 200 mm), (100 mm × 100 mm × 500 mm), and (150 mm × 64 mm), respectively. Following the casting process, the specimens were kept at an ambient temperature of 26 ± 1.5 °C and a relative humidity of 55% for one day. Subsequently, the concrete specimens were de-molded and immersed in water for 7 days according to the ASTM C192 [40] procedure. After this period, they were maintained under the same laboratory conditions until testing was conducted.

2.3. Tests Procedure

In accordance with ASTM C109 [41], ASTM C496 [42], ASTM C78 [43], and ASTM C469 [44], the MRCs' CS, TS, FS, and MOE were assessed. Concrete specimens prepared without the inclusion of DSRTs served as control samples to evaluate the effect of DSRTs content on the proposed concrete strength properties. The average values from three specimens at curing ages of 3, 7, 14, 28, 56, and 90 days were used to evaluate the strength performance, including CS, TS, FS, and MOE. For the compressive and tensile strength tests, an eco-smart automatic machine with maximum load of 3000 kN was used. A constant rate of loading (5 kN/s) was applied until failure of the specimens occurred. The flexural strength test was carried out using the universal testing machine that is used for the determination of the concrete compressive and splitting tensile strength, with a 0.2 kN/s rate of loading. For the MOE test, the specimens were placed between the upper and the lower bearings of the compression testing machine with the sensing device (strain gauge) connected to the monitoring device by the means of data logger. The specimen was loaded to 33% of its failure load so as to ensure that the loading only occurred within the elastic range. Readings from the sensing devices were taken at suitable intervals between 5 kN and 225 kN, and then the load was released. To calculate the water absorption of prepared MRCs specimens, the concrete cubes were immersed in the water for one day, then the weight of specimens was taken. Subsequent to saturation, all MRC specimens were dried in a ventilated oven at 105 °C for over three days, then they were weighed. Then, the total water absorption of tested specimens was calculated using the measured weights of the tested concrete cubes.

To evaluate the microstructural performance of modified binders, cement paste samples made of OPC and MK10 were prepared. XRD, TGA, and DTG tests were conducted after 28 days of curing ages. In accordance with ASTM C1585 [45], the porosity of the proposed MRCs were assessed using water absorption test. This test was conducted at 28 and 90 days of curing age, and an average value of three tested cubes was considered for each age of the evaluated concrete mixtures.

To measure the IR of the proposed MRCs and assess the enhancement in ductility performance, three disc-shaped MRC specimens, each measuring 150 mm × 64 mm, were cut from a cylindrical sample with dimensions of 150 mm × 300 mm for testing. According to ACI committee ACI 544.2R-89, the test was conducted. As shown in Figure 3, the samples were secured using four positioning lugs on a base plate to prevent movement while being struck by a sledgehammer weighing 4.45 kg. The sledgehammer was dropped repeatedly from a height of 457 mm onto a stainless steel ball with a diameter of 635 mm positioned at the center of the concrete disk's top face. The number of blows needed to produce the first crack and the failure of the concrete specimen was recorded. The number of blows needed to produce the first crack (N_1) was noted as the initial crack strength, while the failure strength corresponded to the number of blows resulting in the final failure of the specimen (N_2).

The impact energy at initial crack (IIE_i) was calculated using Equation (1).

$$IIE_i = N_{1i}mgh \quad (1)$$

Likewise, the following equation (Equation (2)) was considered to calculated the ultimate crack impact energy (UIE_u):

$$UIE_u = N_{2u}mgh \quad (2)$$

where N_1 and N_2 are the numbers of blows at the initial and ultimate crack stage, m is the mass of the hammer (4.5 kg), g is gravity acceleration (9.81 m/s^2), and h is the releasing height of the drop hammer (450 mm).

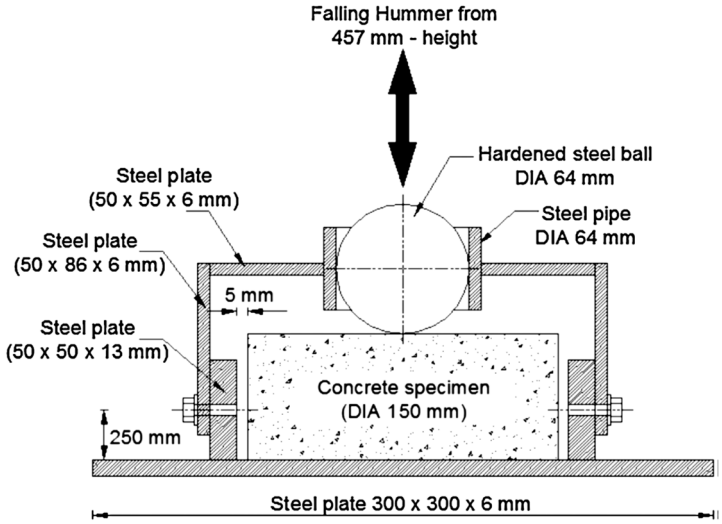

Figure 3. Adopted test to measure the IR of the proposed MRCs [24].

3. Results and Discussion

3.1. Effect of GBFS and MK Content on CS Development

Compared to control specimens (OPC), six mixtures were prepared to evaluate the effect of replacing 30% of OPC with GBFS-MK on MRCs performance. Figure 4 displays the obtained CS at ages of 3, 7, 14, 28, 56, and 90 days. From the obtained results, it can clearly be seen that the inclusion of GBFS and MK in the OPC matrix significantly enhanced the bond strength between the DSRTs surface and modified ternary blended pastes, leading to improved strength performance. However, the significant effects of GBFS and MK on strength development were observed only after 28, 56, and 90 days of curing ages. It is well known that the inclusion of pozzolanic materials in cement matrix leads to slower hydration process at early ages. Specially, when 20% of OPC was replaced by GBFS, the obtained CS results at 3, 7, 14, 28, 56, and 90 days of age were 21.8, 32.2, 37.2, 44.3, 47.9, and 51.2 MPa, respectively, compared to 24.4, 29.8, 35.2, 41.2, 42.1, and 44.8 MPa of OPC specimens.

The inclusion of 5, 10, 15, 20, and 25% MK as OPC replacement in the ternary blended matrix significantly affects the hydration process at an early age and leads to lower strength performance. At 3 days, the substitution of OPC binder with 5–25% MK contributed to a decrease in strength, with the CS of the proposed MRCs dropped from 21.8 MPa to 19.7, 18.6, 17.9, 17.1, and 16.5 MPa, respectively. A similar trend was observed after 7 days of curing age, where the inclusion of 5–25% MK in the cement matrix resulted in a drop in CS to 28.3, 27.8, 25.9, 24.7, and 24.2 MPa in comparison to 32.2 MPa. With an increase in the curing age to 14 days, the loss of strength slightly decreased, and the specimens showed better performance compared to results at 3 and 7 days. Compared to 37.2 MPa,

the inclusion of 5, 10, 15, 20, and 25% MK led to strengths of 36.6, 34.9, 31.2, 29.6, and 28.3 MPa, respectively.

At late ages of 28, 56, and 90 days, the specimens prepared with 10% of MK displayed excellent performance, leading to a significant increase in CS compared to control specimens. At 28 days of age, the specimens prepared with 5, 10, 15, 20, and 25% MK achieved 45.1, 46.4, 40.2, 36.8, and 35.1 MPa, respectively, compared to 44.3 MPa. Likewise, the results at 56 days of age showed a significant improvement in CS development. The average values of CS increased from 47.9 MPa to 49.1 and 50.3 MPa with addition of 5% and 10% MK, respectively. However, the increasing level of replacement up to 15% led to a decrease in CS to 44.9, 40.7, and 38.2 MPa, respectively. Similarly, the specimens subjected to CS test after 90 days of curing age achieved enhancement in CS at 5 and 10% of MK level of replacement, recording values of 53.1 and 55.2 MPa compared to 51.2 MPa for the control specimens. However, increasing the level of replacement to 15, 20, and 25% resulted in a reduction in strength performance, with CS values dropping to 48.6, 43.1, and 40.3 MPa, respectively.

Studies by Sahani et al. [46], Mhaya et al. [22], Bai et al. [47], Sam et al. [48], and Usman et al. [27] have reported that the use of GBFS or MK as SCMs in the cement matrix significantly improves the content of aluminosilicates, generating more dense gels such as C-(A)-S-H, which enhances the CS after 7 days of curing. Additionally, pore size distributions increased with longer curing times [49,50], consistent with earlier studies [51,52]. To optimize strength, it is suggested that the optimal GBFS or MK content is approximately 30% or less of the binder mass. Furthermore, the fineness, activity indices [46,53], and chemical compositions of the GBFS in the studied mixes were responsible for the observed enhancement in CS [34,54].

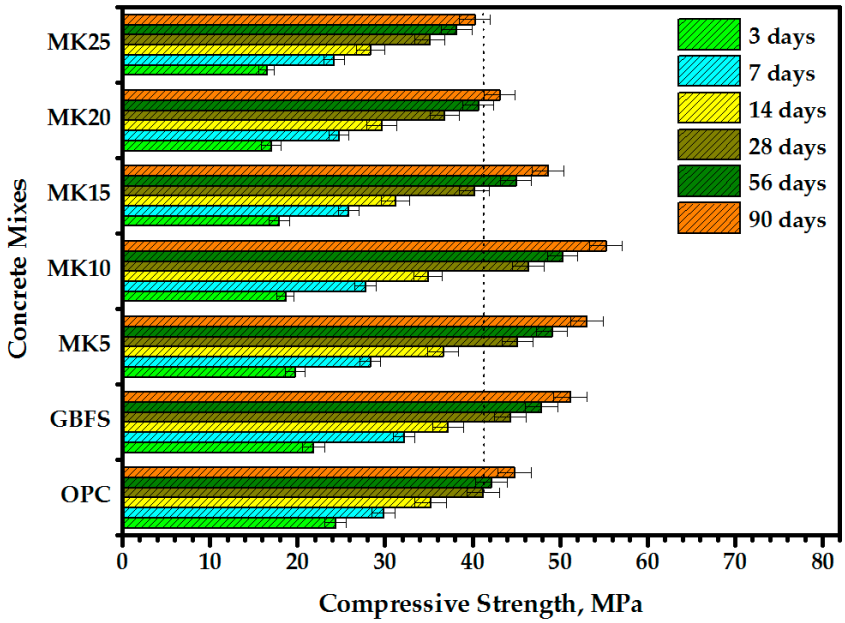

Figure 4. The CS development of MRCs containing GBFS and various levels of MK as OPC replacement after 3, 7, 14, 28, 56, and 90 days of curing age.

3.2. Effect of DSRTs Content on CS of Proposed MRCs

Figure 5 illustrates the obtained results of MRC CS, containing varying amount of DSRTs as NA,s fine or/and coarse replacement. The development of CS in the proposed concrete was assessed at 3, 7, 14, 28, 56, and 90 days of age. In general, the results show that the CS of tested MRC specimens is significantly influenced by DSRT content and the loss in strength tended to increase with increasing DSRTs content in the proposed concrete matrix. As shown in Figure 5a, when DSRTs were used as river sand replacement at levels of 5, 10, 15, 20, and 25%, the early CS at 3 days of age decreased from 18.6 MPa to 17.7,

15.3, 14.4, 10.9, and 10.1 MPa, respectively. Likewise, the obtained results at 7 and 14 days of curing ages dropped to 17.8 and 23.8 MPa, compared to 27.8 and 34.9 MPa, when the level of DSRTs in the MRC matrix raised from 0% to 25%. However, the proposed concrete specimens after 28, 56, and 90 days of age achieved CS higher than 30 MPa and displayed 30.4, 34.1, and 37.7 MPa, making the concrete suitable for industrial applications. The inclusion of DSRTs in the concrete matrix as coarse NAs replacement resulted in a drop in CS values when increasing the amount of replacement from 0% to 5, 10, 15, 20, and 25% (Figure 5b). At 3 days of age, replacing the coarse NAs with 5–25% of DSRTs resulted in a drop in CS reading from 18.6 MPa to 18.1, 16.2, 14.1, 11.9, and 10.3 MPa, respectively. Likewise, the specimens subjected to CS test after 7 and 14 days showed a significant loss in strength performance when increasing the DSRTs content to 25%. After 28 days of curing age, all the MRCs specimens displayed CS of more than 30 MPa; increasing the content of DSRTs in the matrix from 0% to 5, 10, 15, 20, and 25% led to a decrease in the strength value from 46.4 MPa to 43.2, 38.9, 37.2, 32.3, and 30.1 MPa, respectively. Similarly, the evaluated specimens at 56 and 90 days of age and containing 25% of DSRTs as coarse NAs replacement achieved 33.6 and 35.9 MPa, respectively. In the literature, many studies [16,55,56] have indicated that the smooth surface of DSRTs, compared to the rough surface of NAs, reduces the bond strength between the cement paste and the rubber. This reduction in bond strength leads to decreased overall strength as the content of rubber aggregates increases. Similar findings have been reported in previous works [57–59], which demonstrate that DRTCs negatively impact the development of compressive strength (CS).

To evaluate the MRCs' CS performance when NAs are replaced by fine and coarse DSRTs (in a ratio of 50:50), five levels of replacement were considered (5, 10, 15, 20, and 25%), as shown in Figure 5c. At an early age (3 days), the results showed that the inclusion of fine and coarse DSRTs in the concrete matrix to replace 5, 10, 15, 20, and 25% of NAs led to a decrease in CS values from 18.6 MPa to 17.1, 14, 11.1, 10.6, and 9.7 MPa. A similar trend was observed at 7 days, with most MRCs displaying lower strength performance (25.2, 22.4, 19.8, 17.2, and 15.9 MPa) compared to the control specimens (27.8 MPa). However, a slight improvement in CS performance was found after 14 days of age, where the addition of 5, 10, 15, 20, and 25% of DSRTs led to a decrease in the strength from 34.9 MPa to 31.9, 30.1, 27.8, 24.1, and 23.2 MPa, respectively. Significant improvements were observed after 28, 56, and 90 days, and all the prepared MRCs mixtures achieved CS values higher than 30 MPa. At 28 days of age, the inclusion of 5, 10, 15, 20, and 25% of fine and coarse DSRTs resulted in a reduction in CS, and the values dropped from 46.4 MPa to 40.8, 37.8, 35.6, 33.2, and 31 MPa, respectively. Similarly, the CS values of specimens subjected to strength test at 56 days of age dropped to 46.4, 44.2, 39.8, 36.5, and 34.2 MPa compared to 50.3 MPa. In comparison to control specimens (55.2 MPa), specimens evaluated at 90 days of age displayed CS of 49.8, 47.4, 44.1, 41.9, and 36.7 MPa when increasing the replacement of NAs by fine and coarse DSRTs to 5, 10, 15, 20, and 25%, respectively. In a study conducted by Gesoglu et al. [60], the authors recognized that an increase in the amount of DSRTs in the MRC matrix as NAs can lead to a greater loss of CS in the evaluated MRC concretes.

In summary, the decline in the CS values of the proposed MRCs is attributed to multiple factors [56]. First, the aggregate is encased in OPC paste that includes rubber particles. It is evident that cement paste containing fine or/and coarse DSRTTs is softer compared to those without any DSRTs. Cracks can rapidly develop around the rubber particles under load, leading to concrete failure. Second, the presence of inadequate bonds between the rubber particles and the cement paste, compared to the stronger bonds formed between cement paste and natural aggregates, may also result in failure. Third, cracks can develop due to nonuniform stress distributions. Fourth, the physical and mechanical properties of the concrete constituents impact the CS properties. Generally, the CS of concrete decreases when certain components are replaced by rubber particles. Fifth, the low specific gravity of the rubber particles and their weak bonding with other concrete constituents can reduce the CS. These factors indicate that during vibration, the rubber often moves upwards, resulting in higher rubber content in the top layer compared to

other regions of the concrete. In summary, the lack of uniform distribution of concrete constituents is responsible for the drop in designed MRC CS.

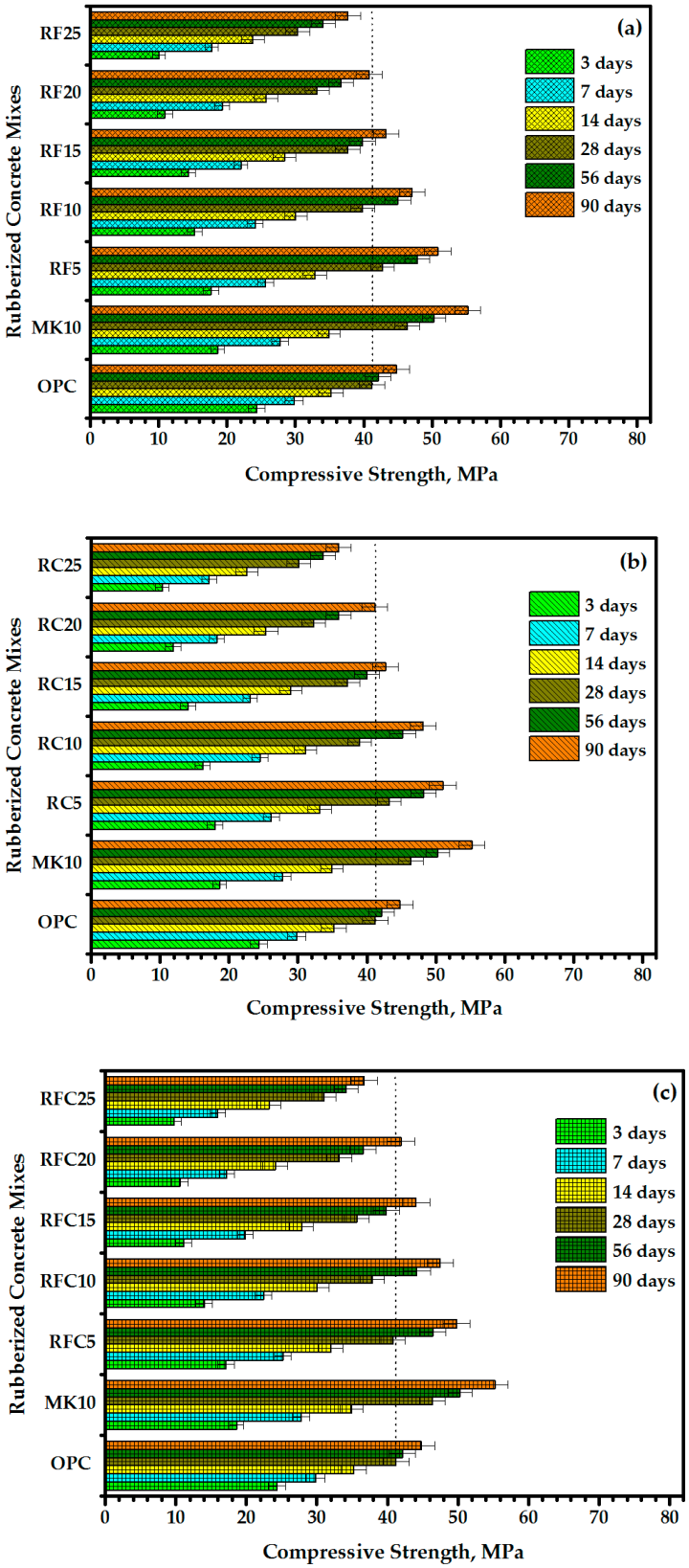

Figure 5. Effect of DSTRs content as NAs replacement on proposed concrete CS development: (**a**) RF5-25, (**b**) RC5-25, and (**c**) RFC5-25.

3.3. X-ray Diffraction (XRD) Patterns Analysis

The XRD analyses of modified cement pastes, in which 30% of OPC is replaced with 20% of GBFS and 10% of MK by weight, are shown in Figure 6. The impact of GBFS and MK on the cement matrix is evident in the 16.2° to 34.8° range, with increased peak intensities of quartz (SiO_2) and albite ($NaAlSi_3O_8$)—gismondine ($CaAl_2Si_2O_8{\cdot}4(H_2O)$). A broad, diffused background peak, peaking around 23.6°, arises from the short-range order of hydrotalcite ($Mg_6Al_2CO_3OH_{16}{\cdot}4H_2O$). The inclusion of GBFS and MK resulted in a higher dense gel peak intensity at 27.9°. Additionally, the mullite peak ($Al_6Si_2O_{13}$) intensity at 14.1° increases with higher GBFS levels. For MK10 matrix, the intensities of C_2S and C_3S peaks at 39.8°, 43°, 44°, 52°, and 56° also increase. Moreover, dense gels such as calcium carbonate ($CaCO_3$), gismondine, and other dense gel products increase with higher GBFS-MK levels. Consequently, the MRCs cube's CS improves from 41.2 MPa to 46.4 MPa at 28 days of curing age. Previously, several studies conducted by Samadi et al. [61] and Baghban et al. [62] have reported that GBFS inclusion can lead to more C-S-H gel production and enhanced calcite formation.

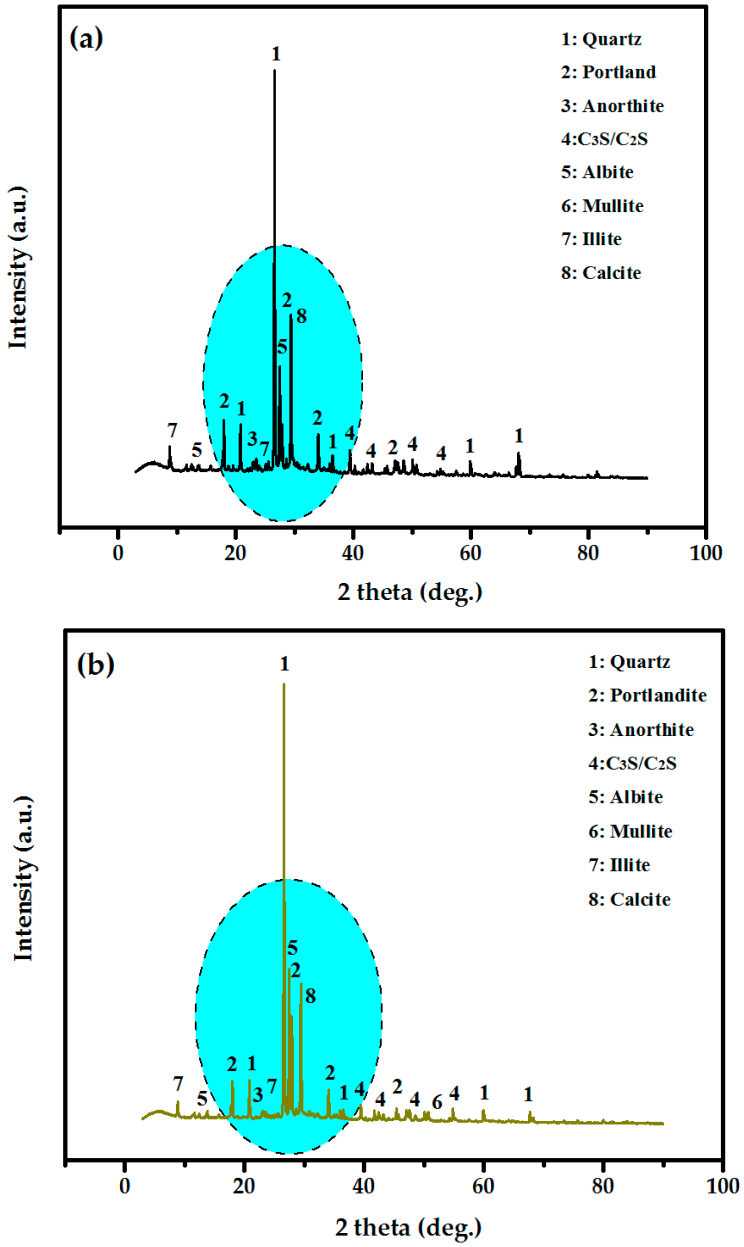

Figure 6. XRD analysis results of modified cement pastes at 28 days of curing age: (**a**) OPC, (**b**) MK10.

The XRD analysis demonstrated the effect of SiO_2, Al_2O_3, and CaO on the CS of the MRC specimens through the formation of C-(A)-S-H gel. Match software version 3.9.0.158 was employed in the XRD measurement to verify the disordered phase of the proposed binders (OPC-GBFS-MK). According to the XRD analysis results (Table 3), the amount of Portlandite decreased from 14.2% to 10.6% as the GBFS and MK content increased from 0% to 30%. The concentration of dense gels, such as calcite and gismondine, increased with the addition of GBFS and MK as a replacement for OPC. It is known that the OPC is essential for C-S-H gel production, and its reduction promotes the formation of dense gels, indicating that the process of dense gel formation from OPC is accelerated with the GBFS and MK matrix compared to OPC specimens. However, a lower content of calcite and albite–gismondine resulted in weaker bonds within the concrete matrix, leading to reduced strength. On the other hand, the high fineness and chemical composition of the GBFS directly affected hydration and silicate and aluminum dissolution, thereby producing higher strength.

Table 3. Element weight % from XRD analysis.

Index	Amount, %				
	Quartz	**Portlandite**	**Calcite**	**Albite and Gismondine**	**Others**
OPC	65.9	14.2	11.7	5.5	2.7
MK10	67.7	10.6	12.5	7.8	1.4

3.4. Thermogravimetric Analysis

Figure 7 presents the TGA and DTG results for modified ternary binders prepared with 0% and 30% GBFS-MK as a replacement for OPC. The sample with 30% GBFS-MK substitution exhibited lower weight loss (10.24%) and greater stability than the control sample (above 14.17%). Additionally, the concentration of C-S-H gels in the modified binder with 30% GBFS-MK was 9.07%, compared to 6.87% for the control sample of OPC. The estimated amount of Portlandite was highest in the OPC (14.18%) compared to 10.27% in the concrete containing 30% GBFS-MK. The enhanced stability of the ternary binders with 30% GBFS-MK can be attributed to the higher content of dense gels such as albite–gismondine ($CaAl_2Si_2O_8{\cdot}4(H_2O)$), calcite ($CaCO_3$), calcium-silicate-hydrate (C-S-H), and calcium-aluminum-silicate-hydrate (C-A-S-H), and lower amount of Portlandite ($Ca(OH)_2$). These findings highlight the benefits of using pozzolanic materials of GBFS and MK as a partial substitute for OPC in improving the microstructure and strength of the studied binders. Jiang et al. [52] reported that hydration products can densify the matrices of bulk pastes, increasing the mechanical properties and durability of concrete and mortars with less than 30% GBFS. The amounts of Portlandite and dense gels in the prepared modified ternary binders were estimated using Equations (3) and (4).

$$\text{Dense gels, \%} = \text{Total LOI} - \text{LOI}_{\text{CH}} - \text{LOI}_{\text{CC}} \quad (3)$$

where LOI(CH) is the dehydration of $Ca(OH)_2$ in the rage of 400 to 550 °C, and LOI(CC) is the CO_2 loss in the range of 600 to 750 °C.

$$\text{Portlandite, \%} = \text{WL}_{\text{CH}}\ (\%) \times [\text{MW}_{\text{CH}}/\text{MW}_{\text{H}}] \quad (4)$$

where WL(CH) is the weight loss due to the CH dehydration, MW(CH) is the molecular weight of CH (74 $g{\cdot}mol^{-1}$), and MW(H) is the molecular weight of water (18 $g{\cdot}mol^{-1}$).

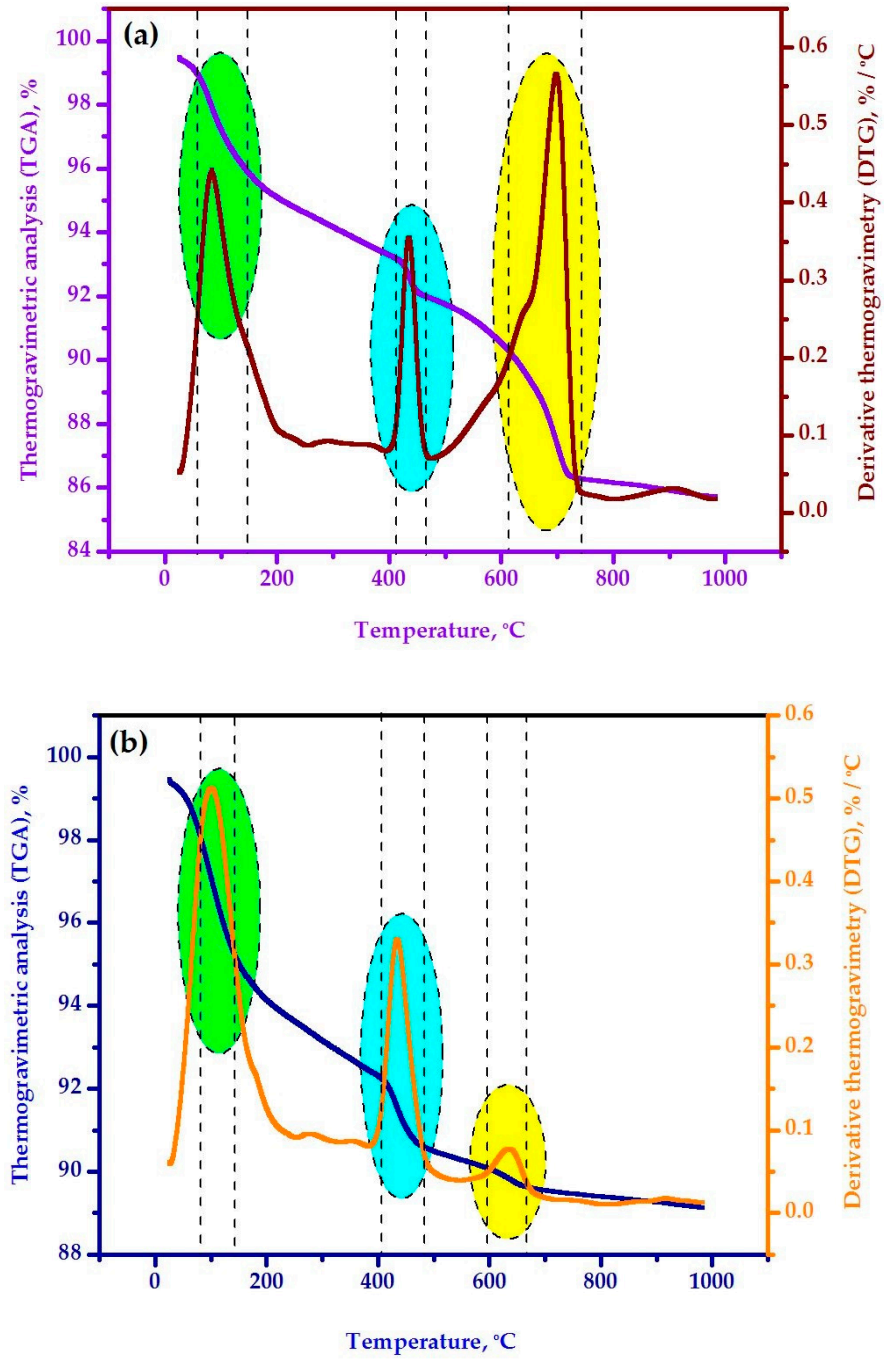

Figure 7. TGA and DTG analysis results of modified binders at 28 days of curing age: (**a**) OPC, (**b**) MK10.

3.5. Effect of Rubberization on Tensile Strength

The effects of GBFS, MK, and DSRTs on the tensile strength (TS) of proposed MRCs were evaluated through the testing. The average TS reading of specimens at ages of 28 and 90 days are illustrated in Figure 8. The results indicate that replacing 30% of cement with GBFS and MK significantly enhanced the TS of MRC specimens. The TS values increased from 2.88 and 3.11 MPa to 3.37 and 3.56 MPa after 28 and 90 days of age, respectively. However, the inclusion of DSRTs in the MRC matrix, either as fine or/and NAs replacement, resulted in a loss of TS. An inverse relationship was observed between the TS and DSRTs content. For the cylinder MRC specimens casted with DSRTs as fine NAs replacement and subjected to TS test at the age of 28 days, increasing the level of replacement from 0% to 5, 10, 15, 20, and 25% led to a decline in TS values from 3.37 MPa to 3.07, 2.82, 2.67, 2.51, and

2.23 MPa, respectively. A similar trend was observed after 90 days of age, with TS readings decreasing from 3.56 MPa to 3.28, 3.14, 2.94, 2.76, and 2.53 MPa as the DSRTs content increased from 0% to 25%. The effect of coarse DSRTs on the TS performance of MRCs was also assessed at 28 and 90 days of age. It was found that for both ages, increasing the content of DSRTs to 25% as crushed stone aggregates replacement significantly led to more loss of TS of tested specimens. At the age of 28 days, the inclusion of 5, 10, 15, 20, and 25% of DSRTs resulted in a drop in TS values from 3.37 MPa to 3.15, 2.91, 2.79, 2.32, and 2.18 MPa. Likewise, the tested specimens after 90 days showed a decrease in TS values from 3.56 MPa to 3.31, 3.17, 3.02, 2.84, and 2.69 MPa with increasing DSRTs content from 0% to 25%. Finally, the effect of DSRTs (in a 50:50 ratio) as fine and coarse NAs replacement was examined after 28 and 90 days, and the results showed similar performance. As the DSRTs replacement level increased, the loss of TS values increased. For the MRC specimens subjected to TS test after the age of 28 days, there was a drop in obtained average readings of TS from 3.37 MPa to 2.82, 2.65, 2.37, 2.29, and 2.24 MPa as the content of fine and coarse DSRTs increased from 0% to 5, 10, 15, 20, and 25%, respectively. A similar trend in obtained readings was found at 90 days of age, and an increasing level of DSRTs from 0% to 25% led to an in increase in the loss of TS values and a drop in the readings from 3.56 MPa to 3.23, 3.16, 3.08, 2.87, and 2.52 MPa. The failure of the specimens at an early curing age was attributed to weak bonding between the rubber aggregates and cement pastes [63]. Additionally, the characteristics and quantity of rubber particles contributed to this failure, as the high deformation of rubberized particles resulted in very low stiffness [56,64]. Consequently, the rubber aggregates behaved like cavities, increasing the stress on their outer perimeter and leading to a reduction in the splitting tensile strength of the specimens under study.

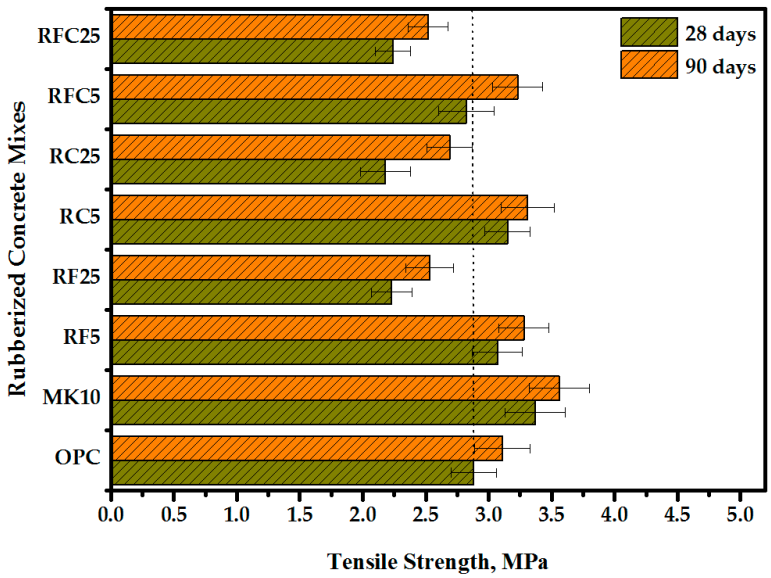

Figure 8. TS of MRCs containing GBFS, MK, and fine and coarse DSRTs at 28 and 90 days of curing age.

3.6. Flexural Strength

Figure 9 illustrates the flexural strength (FS) results of the proposed MRCs containing GBFS, MK, and DSRTs after 28 and 90 days of curing age. The results indicate that replacing 30% of cement binder by 20% of GBFS and 10% of MK significantly enhanced the FS of the MRC specimens, increasing the FS values from 5.62 and 6.02 MPa to 6.16 and 6.82 MPa after the ages of 28 and 90 days, respectively. However, the addition of DSRTs as a replacement for fine or/and NAs led to a noticeable reduction in strength, especially with high amounts of DSRTs (25%). An inverse relationship was observed between the FS and DSRTs content. For the beam specimens prepared with DSRTs as fine NAs replacement and subjected to FS test at the age of 28 days, increasing the level of replacement from 0% to 5, 10, 15, 20, and

25% resulted in a decrease in FS values from 6.16 MPa to 5.75, 5.41, 5.02, 4.48, and 3.98 MPa. A similar trend was observed after the age of 90 days, with FS values decreasing from 6.82 MPa to 6.42, 6.18, 5.71, 5.38, and 5.11 MPa with 5–25% DSRTs inclusion in the MRC matrix. The effect of coarse DSRTs on the FS performance of MRCs at 28 and 90 days of age was also assessed. It was found for both ages that increasing the content of DSRTs to 25% as crushed stone aggregates replacement significantly increased the FS loss in the tested MRC specimens. At the age of 28 days, the inclusion of 5, 10, 15, 20, and 25% of DSRTs resulted in a decrease in FS values from 6.16 MPa to 5.83, 5.24, 5.11, 4.08, and 3.87 MPa, respectively. Likewise, the tested specimens after 90 days showed a decrease in FS values from 6.82 MPa to 6.56, 6.22, 5.66, 5.54, and 4.92 MPa as the DSRTs amount increased from 0% to 25%. Finally, the effect of DSRTs with a 50:50 mix of fine and coarse DSRTs as replacement for fine and coarse NAs was examined after 28 and 90 days. The results showed a similar trend: as the DSRTs replacement level increased, the FS values continued to decrease. The MRC specimens subjected to FS test after the age of 28 days showed a decline in FS values from 6.16 MPa to 5.43, 5.17, 4.94, 4.38, and 4.15 MPa as the content of fine and coarse DSRTs increased from 0% to 5, 10, 15, 20, and 25%, respectively. A similar trend was observed at the age of 90 days: increasing the level of DSRTs from 0% to 25% led to a decrease in FS values from 6.82 MPa to 6.27, 6.12, 5.96, 5.45, and 5.04 MPa, respectively. Overall, the FS values were consistent with CS values, suggesting that significant deformation in the rubber aggregates may have inhibited crack propagation within the concrete matrix. Other researchers [55] have also noted the increased loss in MRC FS readings with higher DSRTs content. The main reason for the decrease in FS values is likely due to the very low adhesion between the rubber crumbs and OPC-GBFS-MK pastes in the concrete matrix, where the rubber particles create free space in the network, thus reducing the density of the concrete [56,65]. Additionally, the smooth surfaces of the rubber particles result in low adhesion with the cement paste [66,67]. The development of tensile stress along the adjacent surfaces of the rubber particles and OPC-GBFS-MK paste due to compressive stress application can lead to premature cracks in modified concretes [57]. This stress originates from the softness of the cracks within the rubber crumbs that begin at the interface of the rubber particles and cement paste and quickly spread throughout the entire concrete matrix, causing failure. A notably wide and weak interfacial transition zone (porous) was observed in DSRTs-included mixes due to the hydrophobic nature of the rubber crumbs, which tend to repel the cement paste [68].

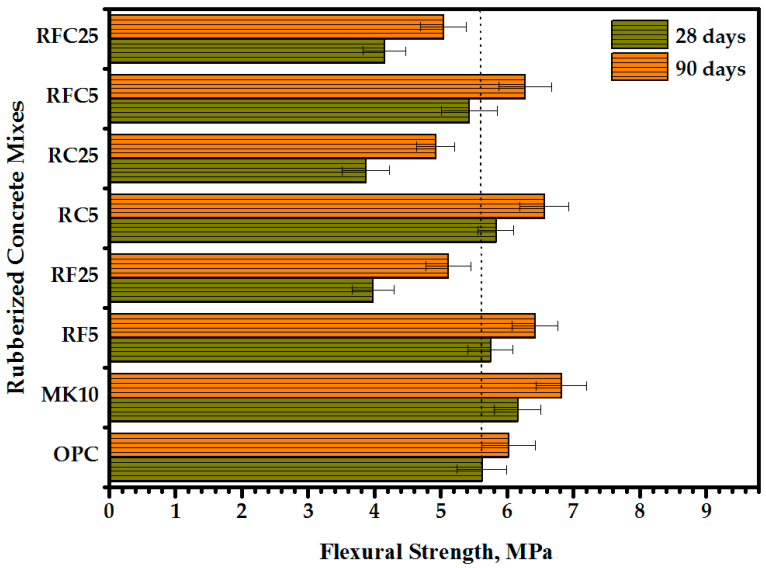

Figure 9. FS of designed MRCs containing DSRTs as fine and coarse NAs replacement after 28 and 90 days of age.

3.7. Modulus of Elasticity (MOE) of Proposed Concrete

The MOE of MRC specimens, prepared with varying levels of DSRTs as fine and coarse NAs replacement, was evaluated and the obtained results are shown in Figure 10. To modify the concrete MOE, 30% of OPC was replaced by GBFS and MK. The results demonstrated that the modified ternary blend led to an increase in the MOE from 28.8 GPa and 29.1 GPa to 29.4 GPa and 30.5 GPa after 28 and 90 days of curing age, respectively. For all tested specimens containing DSRTs, we observed a direct relationship between the DSRTs content and the loss in MOE values. Firstly, the fine NAs were replaced by 5, 10, 15, 20, and 25% of DSRTs, and it was found the MOE values dropped from 29.4 GPa to 27.9, 27.4, 26.9, 25.1, and 22.3 GPa, then from 30.5 GPa to 30.2, 29.6, 28.1, 27.5, and 26.1 GPa after 28 and 90 days of curing age, respectively. Similarly, replacing coarse NAs by DSRTs resulted in a loss of MOE values. The results obtained after 28 days of age showed that the inclusion of 5, 10, 15, 20, and 25% of DSRTs as crushed stone replacement led to a decrease in the MOE reading from 29.4 GPa to 28.1, 27.1, 26.3, 24.9 and 21.8 GPa, respectively. At the age of 90 days, the results indicated that the added coarse DSRTs in the MRC matrix led to a decrease in the MOE values from 30.5 GPa to 30.3, 30.1, 27.9, 27.7, and 25.4 GPa. The effect of DSRTs as fine and coarse NAs replacement was also evaluated, and the obtained results after 28 days of age indicated a drop in the MOE reading to 27.6, 26.9, 25.6, 25.1, and 22.6 GPa, compared to 29.4 GPa of control specimens. At the age of 90 days, a similar trend of results was observed, and the MOE values decreased from 30.5 GP to 29.9, 29.6, 29, 27.6, and 25.9 GPa when increasing the fine and coarse NAs replacement level by DSRTs from 0% to 5–25%, respectively. It is well known that the MOE of concrete is directly related to CS, TS, and FS. For similar reasons to those discussed in Sections 3.2, 3.5, and 3.7, increasing the DSRTs content in the MRC matrix negatively affected the bond strength between the modified cement (OPC-GBFS-MK) and smooth surface of the rubbers, leading to lower strength performance.

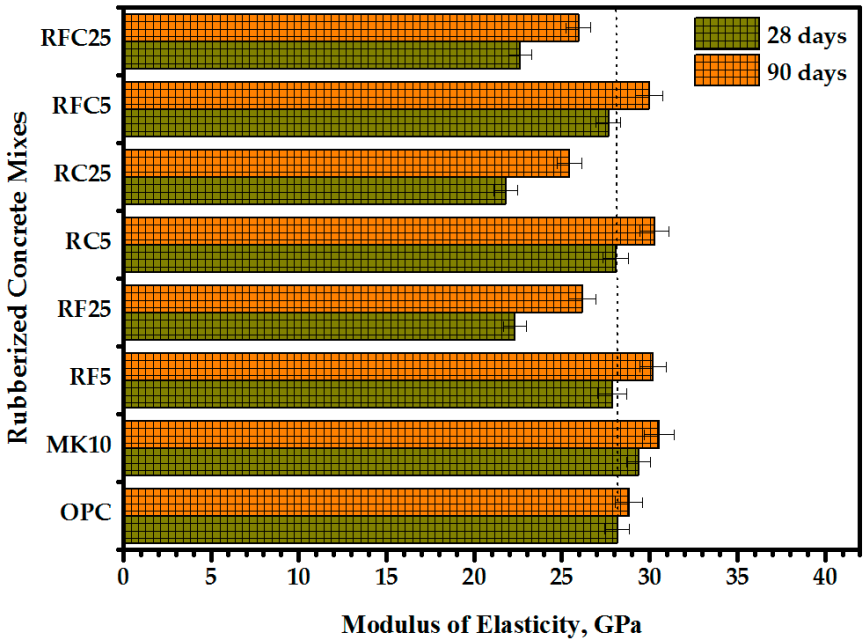

Figure 10. MOE of designed rubberized concrete prepared with various DSRTs content.

3.8. Modified Concrete Porosity

Figure 11 illustrates the effect of GBFS, MK, and various levels of DSRTs inclusion in concrete matrix on the porosity of MRC specimens. The results show that incorporating 30% GBFS-MK as a replacement for OPC positively impacted the microstructure, reducing the pores and leading to lower porosity at 28 and 90 days of age. At the age of 28 days, the porosity decreased from 3.42% to 2.88% when 30% of the OPC was replaced with GBFS

and MK. A similar trend was observed at 90 days of age, with the porosity decreasing from 2.95% to 1.92% as the GBFS-MK content increased from 0% to 30%. The reduction in porosity of the tested MRC specimens is due to the increased density of the concrete, resulting from the formation of additional C-(A)-S-H gels, which significantly reduced the number of pores and cracks. However, the results indicated that the inclusion of DSRTs as fine or/and coarse NAs replacement led to an increase in the porosity of the prepared MRC specimens. For specimens prepared with DSRTs as fine NAs replacement and tested at 28 days of age, the porosity increased from 2.88% to 3.29, 3.66, 3.98, 4.46, and 5.04% when increasing the DSRTs from 0% to 5, 10, 15, 20, and 25%, respectively. Likewise, the specimens assessed after 90 days of age showed an increase in porosity from 1.92% to 2.17, 2.58, 3.05, 3.48, and 3.92% as the DSRTs content increased from 0% to 25%. Similarly, the MRC specimens prepared with DSRTs as a 5–25% replacement for crushed stone led to increased porosity in the 28-day-old specimens from 2.88% to 3.18, 3.86, 4.17, 4.58, and 5.24% and from 1.92% to 2.06, 2.37, 3.26, 3.52, and 4.64% for the specimens evaluated after 90 days of curing age. Finally, the porosity of the MRCs prepared with various levels (5–25%) of DSRTs (50:50) as fine and coarse NAs replacement was measured at 28 and 90 days of age. At the age of 28 days, increasing the content of fine DSRTs from 0% to 5, 10, 15, 20, and 25% resulted in an increment in porosity from 2.88% to 3.53, 3.89, 4.46, 4.73, and 4.95%, respectively. A similar trend was observed at 90 days, with porosity increasing from 1.92% to 2.22, 2.47, 2.85, 3.34, and 4.18% as the fine DSRTs content increased from 5% to 25%. The increment in MRC specimens' porosity containing DSRTs can be attributed to the weak bond between the cement paste and rubber aggregates, resulting in more pores and cracks and high water absorption, which ultimately led to higher porosity readings.

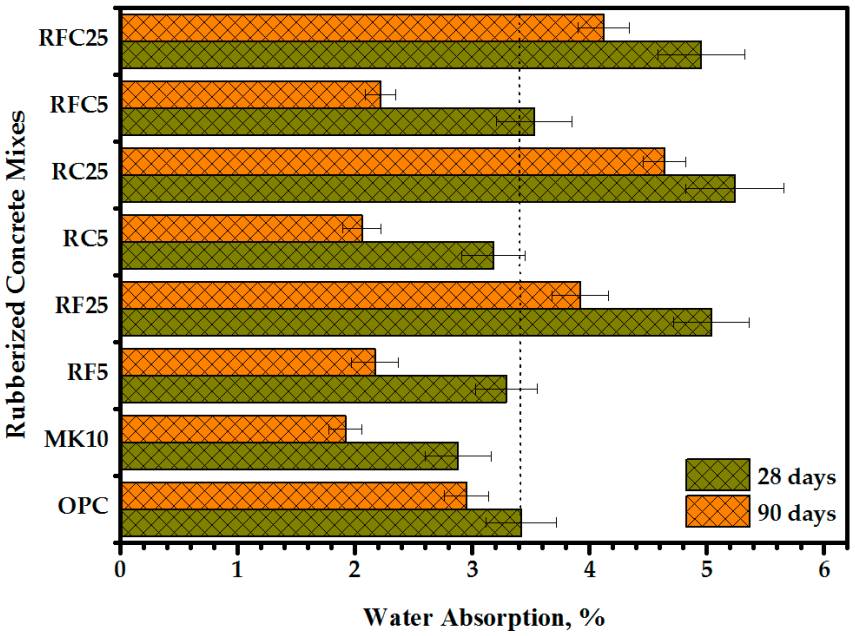

Figure 11. Porosity of prepared MRCs with various levels of fine or/and coarse DSRTs as NAs replacement using water absorption test.

3.9. Impact Resistance

To improve the ductility performance of concrete, MRCs were designed with a ternary blend of OPC-GBFS-MK, along with varying levels (5–25%) of DSRTs as a replacement for fine or/and coarse NAs. The IR test was employed to evaluate the performance of the designed MRC specimens, and the obtained results are presented in Figure 12. The results indicate that the inclusion of GBFS, MK, and DSRTs significantly enhances the ductility of MRC specimens by increasing their resistance to impact loads. Specifically, incorporating 30% GBFS-MK as a replacement for OPC notably increased the number of blows required

to create the initial (N1) and ultimate (failure) cracks (N2) from 14 and 17 blows to 16 and 20 blows, respectively. For the specimens prepared with DSRTs as a replacement for natural fine aggregates, increasing the DSRTs content from 0% to 5, 10, 15, 20, and 25% led to an increase in the required blows of initial cracks from 16 blows to 17, 19, 21, 22, and 24 blows. The number of blows required for ultimate cracks increased from 20 blows to 22, 25, 27, 28, and 31 blows. Similarly, the number of required blows to create the initial and ultimate cracks of specimens prepared with DSRTs as coarse aggregates replacement increased from 16 blows to 18, 20, 23, 24, and 26 blows for the initial cracks and from 20 blows to 23, 26, 29, 32, and 34 blows for the ultimate cracks. Furthermore, specimens prepared with DSRTs as both fine and coarse aggregates replacement showed improvements in IR values, with a direct relationship observed between IR values and DSRTs content. The inclusion of 5, 10, 15, 20, and 25% of DSRTs in the MRC matrix significantly increased the required blows for initial cracks from 16 blows to 19, 21, 22, 24, and 26 blows, and for the ultimate cracks from 20 blows to 23, 26, 29, 31, and 33 blows, respectively. In previous study conducted by Ismail and Hassan [69], the authors observed that replacing 20% NAs with crumb rubber from tire wastes as coarse aggregates positively impacted the proposed concrete's toughness and ductility.

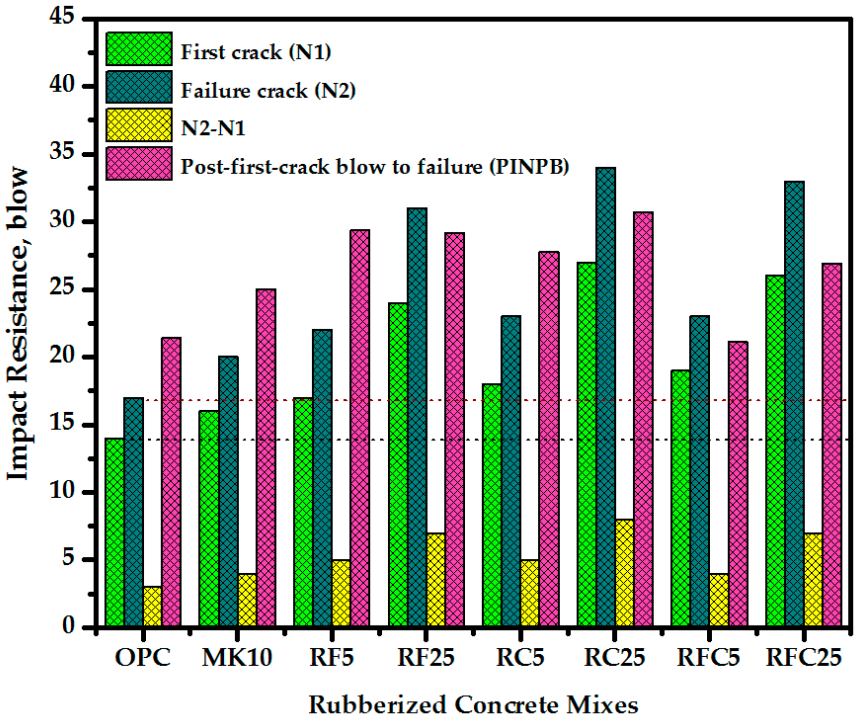

Figure 12. IR of the proposed MRC specimens at 28 days of curing age.

The initial impact energy at first crack (IIE) and ultimate impact energy (UIE) for all MRCs were calculated, and the results are illustrated in Figure 13. Compared to control specimens made of OPC, replacing 30% of the OPC with the combination of GBFS-MK led to an increase in the IIE from 284.35 J to 325.62 J and in the UIE from 345.96 J to 407.02 J. These findings indicate that the impact energy (both first crack and failure) improved as the content of DSRTs in the proposed concrete mixtures increased, whether used as fine or/and coarse aggregate replacement. For the MRC specimens prepared with fine DSRTs as a substitute for river sand, the IIE increased from 325.62 J to 345.96.96.86.67, 427.37, 447.72, and 488.42 J as the substitution content rose from 0% to 5, 10, 15, 20, and 25%. Similarly, the UIE increased to 447.72, 508.77, 549.47, 569.83, and 630.88 J with DSRTs content at the same intervals, compared to 407.02 J for specimens without rubber. Similar results were observed for MRCs designed with coarse DSRTs replacing crushed stone, with both IIE and UIE increasing as the rubber content rose. For IIE, incorporating DSRTs

in MRC mixtures at 5, 10, 15, 20, and 25% increased the energy to 366.32, 404.02, 468.07, 488.42, and 529.12 J, respectively, and corresponding UIE values increased to 468.07, 529.13, 590.18, 651.23, and 691.93 J. The inclusion of DSRTs in a 50:50 ratio as fine and coarse aggregate substitution improved both the IIE and UIE of the MRCs. Replacing river sand and crushed stone with DRTCs at 5, 10, 15, 20, and 25% significantly increased the impact energy from 325.62 J to 386.67, 427.37, 447.72, 488.42, and 529.13 J for the IIE and from 407.02 J to 468.07, 529.13, 590.18, 630.88, and 671.58 J for the UIE. Several studies in the literature [63,64] have reported that replacing NAs with DSRTs increases the load absorption capacity of rubberized concrete and enhances the IR of tested specimens. In a study by Batayneh et al. [70], the authors found that the toughness of rubberized concrete continuously increases with higher rubber content. Experimental work conducted by Taha et al. [57] found that the fracture toughness of rubberized concrete significantly increased with higher DSRTs content, with a 25% replacement of NAs with rubber leading to up to a 132% increase compared to the reference mix. As shown in Figure 14, the linear regression method was used to correlate the experimental data of DSRTs content with UIE; the R^2 values exceeded 0.94 for all samples, indicating strong confidence in the correlation.

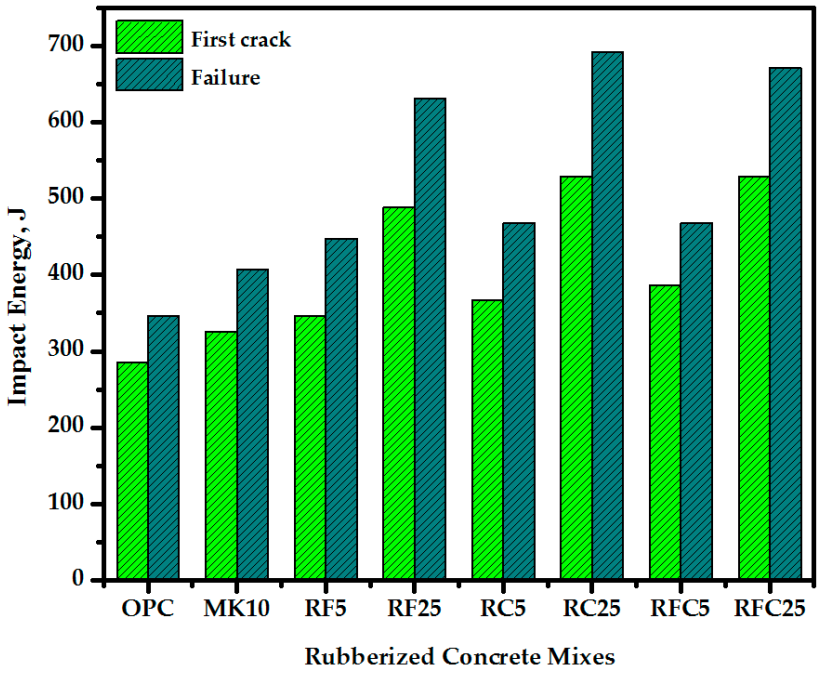

Figure 13. Impact energy of proposed MRCs containing various levels of DSRTs modified with 30% of GBFS-MK as OPC replacement.

Figure 15 shows the crack patterns observed on the MRC disk specimens, which were prepared using DSRTs as replacements for both fine and coarse NAs, and modified with GBFS-MK binders. The inclusion of DSRTs in the proposed MRC mixtures had a positive effect on the IR of the tested specimens. The numerous cracks on the upper surfaces of the MRC disks were a result of the bridging action of the DSRTs, which absorbed more energy and helped prevent unexpected failure. The fractured surfaces of the specimens indicated that the DSRTs were consistently dispersed throughout the disk-shaped concrete specimens.

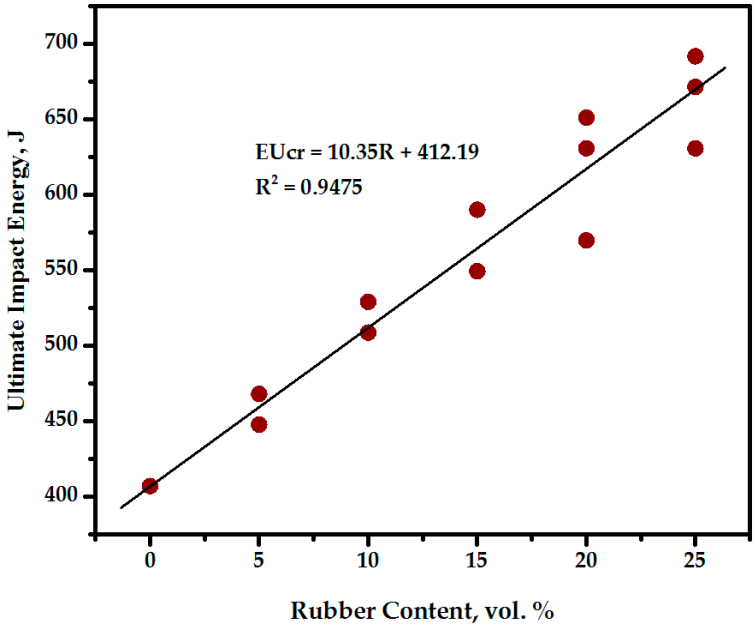

Figure 14. DSRTs content vs. UIE of the proposed MRC specimens.

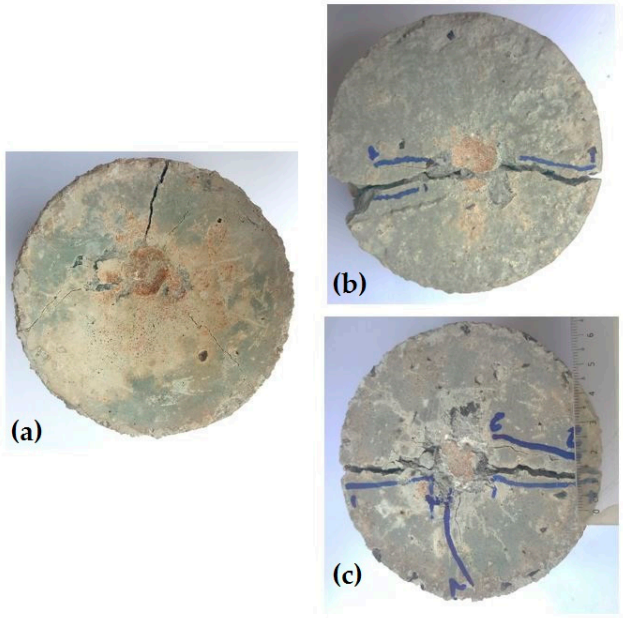

Figure 15. Fracture patterns of MRC disk specimens prepared with various levels of DSRTs and subjected to IR test after 28 days of age: (**a**) MK10, (**b**) RFC5, (**c**) RFC25.

4. Conclusions

The DSRTs were utilized as a replacement for fine or/and coarse NAs in range of 5–25% to improve the ductility performance of proposed MRCs. Ternary blends of OPC-GBFS-MK were adopted to enhance the mechanical and microstructural performance of the designed mixtures. Based on the results obtained, the following conclusions were drawn:

i. The replacement of 30% of OPC with GBFS-MK binders significantly enhanced the bond strength between the modified cement pastes and DSRTs surfaces.
ii. The inclusion of 5, 10, 15, 20, and 25% MK as an OPC replacement in the ternary binder matrix delayed the hydration process, resulting in lower CS at early ages of 3 and 7 days. However, the specimens tested after 28, 56, and 90 days exhibited excellent strength performance.

iii. At 28 days of curing age, the inclusion of 10% MK as an OPC replacement in the OPC-GBFS matrix significantly increased the CS value from 41.2 and 42.3 MPa to 46.4 MPa. This content was selected as an optimal level for preparing the MRC specimens with varying levels of DSRTs.

iv. The results of microstructural analysis (XRD, TGA, and DTG) showed that the inclusion of 30% GBFS and MK as a substitute for OPC positively enhanced the aluminosilicates content and increased the formulation of dense gels. The improvement in the hydration process significantly enhanced the bond strength properties and led to higher CS performance compared to the control specimens.

v. The incorporation of GBFS, MK, and DSRTs into the matrix of the studied MRCs achieved satisfactory CS (up to 30 MPa) after 28 days of curing age, making it advantageous for various applications in the concrete industry.

vi. For the MRC specimens subjected to CS strength testing, it was observed that increasing the DSRTs content, either as fine or/and coarse NAs, in the proposed concrete matrix from 5% to 25% led to a reduction in strength values across all tested ages (3, 7, 14, 28, 56, and 90 days). However, the performance of MRCs after 28 days of age was significantly better than at earlier ages (3–7 days). A similar trend of results was observed for TS, FS, and MOE, where the strength values tended to decrease as the replacement level of NAs with DSRTs increased.

vii. The porosity of MCR specimens was found to be inversely related to the content of DSRTs, with the highest porosity recorded in specimens containing 25% DSRTs as a replacement for NAs.

viii. The inclusion of 5, 10, 15, 20, and 25% DSRTs as replacement for fine or/and coarse NAs significantly enhanced the ductility performance of MRCs by increasing resistance to external impact loads. The highest UIE was achieved with specimens containing 25% DSRTs. It is well known that increasing the DSRTs content in MRC mixtures leads to greater absorption of load, resulting in high IR performance. Additionally, the UIE of the proposed MRCs showed a linear relationship with a high coefficient of determination.

5. Recommendation for Future Investigation

The following areas for further studies are essential for obtaining adequate information on the effectiveness of modified rubberized concrete as construction materials:

i. Durability evaluation: An evaluation of the durability of modified cement containing GBFS and MK with various content of DSRTs is a prerequisite for a wide range of applications in the construction sector.

ii. Bond behavior: The effect of drying shrinkage and creep on the bond behavior between surfaces of rubberized aggregates and modified cement paste should be thoroughly investigated.

iii. Sustainability and environmental impact: Utilizing DSRTs in the concrete industry can significantly reduce landfill problems, fire risks, and the demand for natural aggregates, while also saving cost and energy. It is highly recommended to conduct studies on lifecycle assessment and the environmental benefits of the proposed rubberized concretes.

Author Contributions: Conceptualization, Z.H.J. and B.A.K.; methodology, Z.H.J.; software, B.A.K.; validation, Z.H.J. and B.A.K.; formal analysis, Z.H.J.; investigation, B.A.K.; resources, B.A.K.; data curation, Z.H.J.; writing—original draft preparation, Z.H.J.; writing—review and editing, Z.H.J. and B.A.K.; visualization, B.A.K.; supervision, Z.H.J.; project administration, B.A.K.; funding acquisition, Z.H.J. and B.A.K. All authors have read and agreed to the published version of the manuscript.

Funding: This research received no external funding.

Institutional Review Board Statement: Not applicable.

Informed Consent Statement: Not applicable.

Data Availability Statement: The original contributions presented in the study are included in the article, further inquiries can be directed to the corresponding author.

Acknowledgments: The authors thank University of Misan for their support and cooperation to conduct this research.

Conflicts of Interest: The authors declare no conflicts of interest.

Abbreviations

CS	Compressive strength
DSRTs	Discarded rubber tiers
GBFS	Ground blast furnace slag
IR	Impact resistance
NAs	Natural aggregates
MRCs	Modified rubberized concretes
MOE	Modulus of elasticity
MK	Metakaolin
FS	Flexural strength
TS	Tensile strength
OPC	Ordinary Portlandite cement
IIE	Initial impact energy
UIE	Ultimate impact energy
XRD	X-ray diffraction

References

1. Mirza, J.; Huseien, G.F.; Shah, K.W.; Kirgiz, M.S. Reduction in ecology, environment, economy and energy in concrete industry using waste materials. *J. Adv. Compos. Mater. Constr. Environ. Nano Technol.* **2020**, 1–7.
2. Duthinh, D.; Starnes, M. Strength and Ductility of Concrete Beams Reinforced with Carbon Fiber-Reinforced Polymer Plates and Steel. *J. Compos. Constr.* **2004**, *8*, 59–69. [CrossRef]
3. Pešić, N.; Živanović, S.; Garcia, R.; Papastergiou, P. Mechanical properties of concrete reinforced with recycled HDPE plastic fibres. *Constr. Build. Mater.* **2016**, *115*, 362–370. [CrossRef]
4. Xu, J.; Yao, Z.; Yang, G.; Han, Q. Research on crumb rubber concrete: From a multi-scale review. *Constr. Build. Mater.* **2020**, *232*, 117282. [CrossRef]
5. Khalil, E.; Abd-Elmohsen, M.; Anwar, A.M. Impact Resistance of Rubberized Self-Compacting Concrete. *Water Sci.* **2015**, *29*, 45–53. [CrossRef]
6. Dehdezi, P.K.; Erdem, S.; Blankson, M.A. Physico-mechanical, microstructural and dynamic properties of newly developed artificial fly ash based lightweight aggregate—Rubber concrete composite. *Compos. Part B Eng.* **2015**, *79*, 451–455. [CrossRef]
7. Miller, N.M.; Tehrani, F.M. Mechanical properties of rubberized lightweight aggregate concrete. *Constr. Build. Mater.* **2017**, *147*, 264–271. [CrossRef]
8. Li, L.-J.; Tu, G.-R.; Lan, C.; Liu, F. Mechanical characterization of waste-rubber-modified recycled-aggregate concrete. *J. Clean. Prod.* **2016**, *124*, 325–338. [CrossRef]
9. Liu, F.; Chen, G.; Li, L.; Guo, Y. Study of impact performance of rubber reinforced concrete. *Constr. Build. Mater.* **2012**, *36*, 604–616. [CrossRef]
10. Mhaya, A.M.; Shahidan, S.; Goel, A.; Huseien, G.F. Effect of metakaolin content and shape design on strength performance of lightweight rubberized geopolymer mortars incorporated slag-waste glass powders. *Constr. Build. Mater.* **2024**, *432*, 136500. [CrossRef]
11. Khatib, Z.K.; Bayomy, F.M. Rubberized Portland cement concrete. *J. Mater. Civ. Eng.* **1999**, *11*, 206–213. [CrossRef]
12. Fu, C.; Ye, H.; Wang, K.; Zhu, K.; He, C. Evolution of mechanical properties of steel fiber-reinforced rubberized concrete (FR-RC). *Compos. Part B Eng.* **2019**, *160*, 158–166. [CrossRef]
13. Youssf, O.; Swilam, A.; Tahwia, A.M. Performance of crumb rubber concrete made with high contents of heat pre-treated rubber and magnetized water. *J. Mater. Res. Technol.* **2023**, *23*, 2160–2176. [CrossRef]
14. Eldin, N.N.; Senouci, A.B. Rubber-Tire Particles as Concrete Aggregate. *J. Mater. Civ. Eng.* **1993**, *5*, 478–496. [CrossRef]
15. Al-Fasih, M.Y.M.; Huseien, G.F.; bin Ibrahim, I.S.; Sam, A.R.M.; Algaifi, H.A.; Alyousef, R. Synthesis of rubberized alkali-activated concrete: Experimental and numerical evaluation. *Constr. Build. Mater.* **2021**, *303*, 124526. [CrossRef]
16. Mhaya, A.M.; Huseien, G.F.; Abidin, A.R.Z.; Ismail, M. Long-term mechanical and durable properties of waste tires rubber crumbs replaced GBFS modified concretes. *Constr. Build. Mater.* **2020**, *256*, 119505. [CrossRef]
17. Turatsinze, A.; Bonnet, S.; Granju, J.-L. Mechanical characterisation of cement-based mortar incorporating rubber aggregates from recycled worn tyres. *Build. Environ.* **2005**, *40*, 221–226. [CrossRef]

18. Swilam, A.; Tahwia, A.M.; Youssf, O. Effect of Rubber Heat Treatment on Rubberized-Concrete Mechanical Performance. *J. Compos. Sci.* **2022**, *6*, 290. [CrossRef]
19. Si, R.; Guo, S.; Dai, Q. Durability performance of rubberized mortar and concrete with NaOH-Solution treated rubber particles. *Constr. Build. Mater.* **2017**, *153*, 496–505. [CrossRef]
20. Hossain, F.Z.; Shahjalal, M.; Islam, K.; Tiznobaik, M.; Alam, M.S. Mechanical properties of recycled aggregate concrete containing crumb rubber and polypropylene fiber. *Constr. Build. Mater.* **2019**, *225*, 983–996. [CrossRef]
21. Hesami, S.; Hikouei, I.S.; Emadi, S.A.A. Mechanical behavior of self-compacting concrete pavements incorporating recycled tire rubber crumb and reinforced with polypropylene fiber. *J. Clean. Prod.* **2016**, *133*, 228–234. [CrossRef]
22. M. Mhaya, A.; Baghban, M.H.; Faridmehr, I.; Huseien, G.F.; Abidin, A.R.Z.; Ismail, M. Performance evaluation of modified rubberized concrete exposed to aggressive environments. *Materials* **2021**, *14*, 1900. [CrossRef] [PubMed]
23. Mhaya, A.M.; Shahidan, S.; Zuki, S.S.M.; Huseien, G.F.; Azmi, M.A.M.; Ismail, M.; Mirza, J. Durability and Acoustic Performance of Rubberized Concrete Containing POFA as Cement Replacement. *Sustainability* **2022**, *14*, 15510. [CrossRef]
24. Mhaya, A.M.; Huseien, G.F.; Faridmehr, I.; Abidin, A.R.Z.; Alyousef, R.; Ismail, M. Evaluating mechanical properties and impact resistance of modified concrete containing ground Blast Furnace slag and discarded rubber tire crumbs. *Constr. Build. Mater.* **2021**, *295*, 123603. [CrossRef]
25. Mhaya, A.M.; Baharom, S.; Huseien, G.F. Improved strength performance of rubberized Concrete: Role of ground blast furnace slag and waste glass bottle nanoparticles amalgamation. *Constr. Build. Mater.* **2022**, *342*, 128073. [CrossRef]
26. Huseien, G.F.; Mirza, J.; Ismail, M.; Ghoshal, S.; Ariffin, M.A.M. Effect of metakaolin replaced granulated blast furnace slag on fresh and early strength properties of geopolymer mortar. *Ain Shams Eng. J.* **2018**, *9*, 1557–1566. [CrossRef]
27. Usman, J.; Sam, A.R.M.; Hussin, M.W. Behavior of Palm Oil Fuel Ash and Metakaolin Ternary Blend Cement Mortar at Elevated Temperatures. *J. Mater. Civ. Eng.* **2017**, *29*. [CrossRef]
28. Mansour, A.; Al Biajawi, M. The effect of the addition of metakaolin on the fresh and hardened properties of blended cement products: A review. *Mater. Today Proc.* **2022**, *66*, 2811–2817. [CrossRef]
29. Zhang, H.; Zhang, Q.; Zhang, M.; Tang, S.; Pei, Y.; Skoczylas, F.; Feng, S. Effect of fly ash and metakaolin on the mechanical properties and microstructure of magnesium ammonium phosphate cement paste. *Constr. Build. Mater.* **2024**, *424*, 135871. [CrossRef]
30. Gholampour, A.; Ozbakkaloglu, T. Performance of sustainable concretes containing very high volume Class-F fly ash and ground granulated blast furnace slag. *J. Clean. Prod.* **2017**, *162*, 1407–1417. [CrossRef]
31. Yazıcı, H.; Yardımcı, M.Y.; Yiğiter, H.; Aydın, S.; Türkel, S. Mechanical properties of reactive powder concrete containing high volumes of ground granulated blast furnace slag. *Cem. Concr. Compos.* **2010**, *32*, 639–648. [CrossRef]
32. Wang, X.-Y.; Lee, H.-S. Modeling the hydration of concrete incorporating fly ash or slag. *Cem. Concr. Res.* **2010**, *40*, 984–996. [CrossRef]
33. Tang, S.W.; Cai, R.J.; He, Z.; Cai, X.H.; Shao, H.Y.; Li, Z.J.; Yang, H.M.; Chen, E. Continuous Microstructural Correlation Of Slag/Superplasticizer Cement Pastes By Heat And Impedance Methods Via Fractal Analysis. *Fractals* **2017**, *25*, 17400035. [CrossRef]
34. Pal, S.; Mukherjee, A.; Pathak, S. Investigation of hydraulic activity of ground granulated blast furnace slag in concrete. *Cem. Concr. Res.* **2003**, *33*, 1481–1486. [CrossRef]
35. Huseiena, G.F.; Ismail, M.; Tahir, M.; Mirza, J.; Hussein, A.; Khalid, N.; Sarbini, N. Effect of binder to fine aggregate content on performance of sustainable alkali activated mortars incorporating solid waste materials. *Chem. Eng.* **2018**, *63*, 667–672.
36. Kalina, R.D.; Al-Shmaisani, S.; Ferron, R.D.; Juenger, M.C.G. False positives in ASTM C618 specifications for natural pozzolans. *ACI Mater. J.* **2019**, *116*, 165–172. [CrossRef]
37. *C33/C33M*; Standard Specification for Concrete Aggregates. American Society for Testing and Materials: Philadelphia, PA, USA, 2003.
38. Neville, A.M. *Properties of Concrete*; Longman: London, UK, 1995; Volume 4.
39. *ASTM C136-06*; Standard Test Method for Sieve Analysis of Fine and Coarse Aggregates. American Society for Testing and Materials: Philadelphia, PA, USA, 2006.
40. *C192/C192M*; Standard Practice for Making and Curing Concrete Test Specimens in the Laboratory. American Society for Testing and Materials: Philadelphia, PA, USA, 2007.
41. *C109/C109M*; ASTM C109-Standard Test Method for Compressive Strength of Hydraulic Cement Mortars. ASTM International: West Conshohocken, PA, USA, 2008.
42. *ASTM-C496*; Standard Test Method for Splitting Tensile Strength of Cylindrical Concrete. American Society for Testing and Materials: West Conshohocken, PA, USA, 1996.
43. *ASTM C78/C78M-22*; Standard Test Method for Flexural Strength of Concrete (Using Simple Beam with Third-Point Loading). American Society for Testing and Materials: West Conshohocken, PA, USA, 2010.
44. Voigt, A. Evaluation of Methods for Measuring Concrete Modulus of Elasticity. Master's Thesis, University of Wyoming, Laramie, WY, USA, 2010.
45. *ASTM C1585-20*; Standard Test Method for Measurement of Rate of Absorption of Water by Hydraulic-Cement Concretes. American Society for Testing and Materials: West Conshohocken, PA, USA, 2013.

46. Sahani, A.K.; Samanta, A.K.; Roy, D.K.S. Influence of mineral by-products on compressive strength and microstructure of concrete at high temperature. *Adv. Concr. Constr.* **2019**, *7*, 263–275.
47. Bai, W.; Hu, H.; Yuan, C.; Guan, J.; Xie, C.; Lv, Y. The influence of blast furnace slag on the mechanical properties and mesoscopic damage mechanisms of recycled aggregate concrete compared to natural aggregate concrete at different ages. *J. Build. Eng.* **2024**, *94*, 109926. [CrossRef]
48. Sam, A.R.M.; Usman, J.; Sumadi, S.R. Properties of binary and ternary blended cement mortars containing palm oil fuel ash and metakaolin. *J. Chin. Inst. Eng.* **2017**, *40*, 170–178. [CrossRef]
49. Li, Y.; Chen, Y. Influence of ground mineral admixtures on pore structure of hardened cement paste and strength of cement mortar. *J.-Chin. Ceram. Soc.* **2006**, *34*, 575. [CrossRef]
50. Qiang, W.; Mengxiao, S.; Jun, Y. Influence of classified steel slag with particle sizes smaller than 20 μm on the properties of cement and concrete. *Constr. Build. Mater.* **2016**, *123*, 601–610. [CrossRef]
51. Sun, J. Study of effects of ground steel slag on mechanical performance and soundness of concrete. *Coal Ash. China* **2003**, *15*, 7–9.
52. Jiang, Y.; Ling, T.-C.; Shi, C.; Pan, S.-Y. Characteristics of steel slags and their use in cement and concrete—A review. *Resour. Conserv. Recycl.* **2018**, *136*, 187–197. [CrossRef]
53. Huseien, G.F.; Sam, A.R.M.; Shah, K.W.; Mirza, J. Effects of ceramic tile powder waste on properties of self-compacted alkali-activated concrete. *Constr. Build. Mater.* **2020**, *236*, 117574. [CrossRef]
54. Özkan, Ö.; Yüksel, I.; Muratoğlu, Ö. Strength properties of concrete incorporating coal bottom ash and granulated blast furnace slag. *Waste Manag.* **2007**, *27*, 161–167. [CrossRef] [PubMed]
55. Siddika, A.; Al Mamun, M.A.; Alyousef, R.; Amran, Y.H.M.; Aslani, F.; Alabduljabbar, H. Properties and utilizations of waste tire rubber in concrete: A review. *Constr. Build. Mater.* **2019**, *224*, 711–731. [CrossRef]
56. Ganjian, E.; Khorami, M.; Maghsoudi, A.A. Scrap-tyre-rubber replacement for aggregate and filler in concrete. *Constr. Build. Mater.* **2009**, *23*, 1828–1836. [CrossRef]
57. Taha, M.M.R.; El-Dieb, A.S.; El-Wahab, M.A.A.; Abdel-Hameed, M.E. Mechanical, Fracture, and Microstructural Investigations of Rubber Concrete. *J. Mater. Civ. Eng.* **2008**, *20*, 640–649. [CrossRef]
58. Duarte, A.; Silva, B.; Silvestre, N.; de Brito, J.; Júlio, E.; Castro, J. Tests and design of short steel tubes filled with rubberised concrete. *Eng. Struct.* **2016**, *112*, 274–286. [CrossRef]
59. Mhaya, A.M.; Abidin, A.R.Z.; Sarbini, N.N.; Ismail, M. Role of crumb tyre aggregates in rubberised concrete contained granulated blast-furnace slag. *IOP Conf. Ser. Earth Environ. Sci.* **2019**, *220*, 012029. [CrossRef]
60. Gesoglu, M.; Güneyisi, E.; Hansu, O.; Ipek, S.; Asaad, D.S. Influence of waste rubber utilization on the fracture and steel—concrete bond strength properties of concrete. *Constr. Build. Mater.* **2015**, *101*, 1113–1121. [CrossRef]
61. Samadi, M.; Huseien, G.F.; Mohammadhosseini, H.; Lee, H.S.; Lim, N.H.A.S.; Tahir, M.M.; Alyousef, R. Waste ceramic as low cost and eco-friendly materials in the production of sustainable mortars. *J. Clean. Prod.* **2020**, *266*, 121825. [CrossRef]
62. Baghban, M.H.; Mhaya, A.M.; Faridmehr, I.; Ghasan, F.H. Carbonation Depth and Chloride Ion Penetration Properties of Rubberised Concrete Incorporated Ground Blast Furnace Slag. *Solid State Phenom.* **2022**, *329*, 101–108. [CrossRef]
63. Akinyele, J.O.; Salim, R.W.; Kupolati, W.K. The Impact of Rubber Crumb on The Mechanical and Chemical Properties of Concrete. *Eng. Struct. Technol.* **2015**, *7*, 197–204. [CrossRef]
64. Aslani, F.; Ma, G.; Wan, D.L.Y.; Le, V.X.T. Experimental investigation into rubber granules and their effects on the fresh and hardened properties of self-compacting concrete. *J. Clean. Prod.* **2018**, *172*, 1835–1847. [CrossRef]
65. Aslani, F. Mechanical Properties of Waste Tire Rubber Concrete. *J. Mater. Civ. Eng.* **2015**, *28*. [CrossRef]
66. Thomas, B.S.; Gupta, R.C. Properties of high strength concrete containing scrap tire rubber. *J. Clean. Prod.* **2016**, *113*, 86–92. [CrossRef]
67. Thomas, B.S.; Gupta, R.C.; Panicker, V.J. Recycling of waste tire rubber as aggregate in concrete: Durability-related performance. *J. Clean. Prod.* **2016**, *112*, 504–513. [CrossRef]
68. Gupta, T.; Chaudhary, S.; Sharma, R.K. Assessment of mechanical and durability properties of concrete containing waste rubber tire as fine aggregate. *Constr. Build. Mater.* **2014**, *73*, 562–574. [CrossRef]
69. Ismail, M.K.; Hassan, A.A.A. Performance of Full-Scale Self-Consolidating Rubberized Concrete Beams in Flexure. *ACI Mater. J.* **2016**, *113*, 207–218. [CrossRef]
70. Batayneh, M.K.; Marie, I.; Asi, I. Promoting the use of crumb rubber concrete in developing countries. *Waste Manag.* **2008**, *28*, 2171–2176. [CrossRef] [PubMed]